




REVIEW ARTICLE

Definitions and classification of malformations of cortical development: practical guidelines

 **Mariasavina Severino,¹ Ana Filipa Geraldo,^{1,2} Norbert Utz,³ Domenico Tortora,¹**
 **Ivana Pogledic,⁴ Włodzimierz Klonowski,⁵ Fabio Triulzi,⁶ Filippo Arrigoni,⁷**
Kshitij Mankad,⁸ Richard J. Leventer,⁹  Grazia M.S. Mancini,¹⁰ James A. Barkovich,^{11,12,*}
Maarten H. Lequin,^{13,*} and Andrea Rossi^{1,*} on behalf of the European Network on Brain Malformations (Neuro-MIG)

*These authors contributed equally to this work.

Malformations of cortical development are a group of rare disorders commonly manifesting with developmental delay, cerebral palsy or seizures. The neurological outcome is extremely variable depending on the type, extent and severity of the malformation and the involved genetic pathways of brain development. Neuroimaging plays an essential role in the diagnosis of these malformations, but several issues regarding malformations of cortical development definitions and classification remain unclear. The purpose of this consensus statement is to provide standardized malformations of cortical development terminology and classification for neuroradiological pattern interpretation. A committee of international experts in paediatric neuroradiology prepared systematic literature reviews and formulated neuroimaging recommendations in collaboration with geneticists, paediatric neurologists and pathologists during consensus meetings in the context of the European Network Neuro-MIG initiative on Brain Malformations (<https://www.neuro-mig.org/>). Malformations of cortical development neuroimaging features and practical recommendations are provided to aid both expert and non-expert radiologists and neurologists who may encounter patients with malformations of cortical development in their practice, with the aim of improving malformations of cortical development diagnosis and imaging interpretation worldwide.

- 1 Neuroradiology Unit, IRCCS Istituto Giannina Gaslini, Genoa, Italy
- 2 Neuroradiology Unit, Imaging Department, Centro Hospitalar Vila Nova de Gaia/Espinho (CHVNG/E), Vila Nova de Gaia, Portugal
- 3 Department of Pediatric Radiology, HELIOS Klinikum Krefeld, Germany
- 4 Division of Neuroradiology and Musculoskeletal Radiology, Department of Biomedical Imaging and Image-guided Therapy, Medical University of Vienna, Vienna, Austria
- 5 Nalecz Institute of Biocybernetics and Biomedical Engineering Polish Academy of Sciences, Poland
- 6 Neuroradiology Unit, Fondazione IRCCS Cà Granda, Ospedale Maggiore Policlinico, Department of Pathophysiology and Transplantation, Università degli Studi Milano, Italy
- 7 Department of Neuroimaging Lab, Scientific Institute, IRCCS E. Medea, Bosisio Parini, Italy
- 8 Department of Radiology, Great Ormond Street Hospital for Children NHS Foundation Trust, Great Ormond Street, London, UK
- 9 Department of Neurology Royal Children's Hospital, Murdoch Children's Research Institute and University of Melbourne Department of Pediatrics, Melbourne, Australia
- 10 Department of Clinical Genetics, Erasmus MC University Medical Center, Rotterdam, The Netherlands
- 11 Department of Radiology and Biomedical Imaging, University of California, San Francisco, CA, USA
- 12 Department of Neurology, University of California, San Francisco, CA, USA
- 13 Department of Radiology, University Medical Center Utrecht, Utrecht, The Netherlands

Received October 1, 2019. Revised March 14, 2020. Accepted March 30, 2020. Advance access publication August 10, 2020

© The Author(s) (2020). Published by Oxford University Press on behalf of the Guarantors of Brain.

This is an Open Access article distributed under the terms of the Creative Commons Attribution Non-Commercial License (<http://creativecommons.org/licenses/by-nc/4.0/>), which permits non-commercial re-use, distribution, and reproduction in any medium, provided the original work is properly cited. For commercial re-use, please contact journals.permissions@oup.com

¹Correspondence to: Maarten H. Lequin

Department of Radiology, Wilhelmina Children's Hospital, University Medical Center

Utrecht, Lundlaan 6, 3584 EA Utrecht, The Netherlands

E-mail: M.H.Lequin@umcutrecht.nl

Keywords: malformations of cortical development; classification; epilepsy; neuroimaging

Abbreviations: aRGC = apical radial glial cells; FCD = focal cortical dysplasia; HMEG = hemimegalencephaly; MCD = malformations of cortical development; OFC = occipital-frontal circumference; SBH = subcortical band heterotopia; (S)VZ = (sub)ventricular zone

Introduction

Malformations of cortical development (MCD) comprise a large, heterogeneous group of disorders of disrupted cerebral cortex formation caused by various genetic, infectious, vascular, or metabolic aetiologies (Raybaud and Widjaja, 2011; Barkovich *et al.*, 2012). MCD are characterized by abnormal cortical structure or presence of heterotopic grey matter, sometimes associated with abnormal brain size (i.e. micrencephaly or megalencephaly) (Raybaud and Widjaja, 2011; Barkovich *et al.*, 2012). MCD may cause significant morbidity at any age, but most commonly symptom onset ranges from early childhood to early adult age, manifested as epilepsy, developmental delay, intellectual disability or cerebral palsy (Raybaud and Widjaja, 2011; Barkovich *et al.*, 2012). Notably, it is estimated that ~40–50% of drug-resistant epilepsies treated by surgery in children are caused by MCD (Pasquier *et al.*, 2002).

The definitive diagnosis of MCD is based on neuropathological findings; however, pathological tissue is rarely available except for epilepsy surgery cases or rare cases resulting in autopsy. Therefore, for most practical purposes, diagnosis begins with the neuroimaging features; associated clinical phenotyping and genetic findings aid in subclassification. Despite the abundant literature, several issues regarding the definitions and classification of these malformations remain unclear. Indeed, diagnostic terms for different subtypes of MCD are often used imprecisely, and full agreement concerning their definitions, based on neuroimaging criteria, has yet to be reached. Moreover, classification schemes change constantly (Barkovich *et al.*, 1996, 2001, 2005, 2012) based on new genetic and mechanistic discoveries, while, at the same time, increasing the difficulty in categorizing MCD into well-defined, rigid groups (Barkovich, 2013). An updated, shared terminology and precise classification of MCD would greatly help to improve genotype-phenotype correlations and communication among radiologists, clinicians, pathologists and laboratory geneticists. In addition, greater specificity of neuroimaging pattern descriptions/reports may improve the diagnostic rate by allowing more targeted genetic testing or facilitating discovery of new genotype-phenotype correlations. Finally, the complex nature and high degree of clinical, neuroimaging and genetic heterogeneity of MCD (no two malformations are identical) requires a multidisciplinary approach, as well as substantial expertise

in pattern recognition using brain MRI with high-quality age-specific protocols. Novel digital pathology methods for computer-aided analysis of images may be very helpful in improving detection rate and reducing the human factor in making correct diagnosis of MCD (Klonowski, 2016).

To this end, a large group of MCD experts came together in a pan-European, multidisciplinary network (COST Action Neuro-MIG, www.neuro-mig.org), aiming to improve diagnosis, management and research on MCD (Mancini, 2018). Based on a critical review of the literature, extensive personal experiences, and multidisciplinary discussions, this consensus paper of best practice guidelines for the radiological diagnosis of MCD in the post-natal period was conceived, beginning from an overview of currently accepted classification schemes, including notions of embryological processes and potential classification limits and challenges. Moreover, we provide basic concepts regarding the normal cortical appearance on MRI, a practical approach for imaging diagnosis of MCD, followed by a focus on definitions and relevant neuroimaging features of MCD.

Search strategy and methods

This review represents a consensus document discussed during face-to-face expert meetings within the European Network Neuro-MIG on Brain Malformations (Mancini, 2018). The Neuro-MIG network is a consortium of clinical, genetic, and translational researchers devoted to the study of cortical malformations, with a work package dedicated to the imaging of MCD and development of neuroimaging guidelines and research projects based on advanced MRI techniques [Work Group (WG) 2]. The European Network Neuro-MIG is funded by the COST (European Cooperation in Science and Technology) Action CA16118, which did not influence the content of the present consensus paper.

Five researchers (M.S., N.U., A.F.G., M.L., A.R.) from WG 2 prepared systematic literature reviews in advance of the consensus workshops held on 14 September 2018 in Lisbon, Portugal and 17 March 2019 in Rehovot, Israel. PubMed was systematically queried for phenotypes and imaging features associated with MCD, using the key words 'malformations of cortical development', 'microcephaly', 'micrencephaly', 'brain overgrowth disorders',

‘megalencephaly’, ‘hemimegalencephaly’, ‘lissencephaly’, ‘microlissencephaly’, ‘polymicrogyria’, ‘schizencephaly’, ‘cobblestone malformation’, ‘focal cortical dysplasia’, ‘dysgyria’ and ‘heterotopia’. About 500 articles written in English were included in the review, which was conducted between 10 January 2018 and 15 September 2019. Because of the lack of randomized trials for almost all questions discussed, formalized grading of evidence and recommendations was not performed. Initial recommendations were developed during the workshops via iterative discussion in thematic working groups and plenary sessions. MCD definitions and imaging features were discussed with paediatric neurologists, geneticists, and neuropathologists from two other NeuroMIG working groups (WG1 Clinical Phenotyping, and WG3 Genotyping). A first draft summarizing the consensus recommendations was compiled by three researchers (M.S., N.U. and M.L.) and then reviewed and approved by all members of WG 2. The final version of the consensus document was then circulated among all COST Network members prior to submission. Practical guidelines are provided as [Supplementary material](#), Key points and recommendations.

Classification by stage of developmental disruption

The first classification based on imaging and embryological processes was introduced by [Barkovich *et al.* in 1996](#) and updated in the following years ([Barkovich *et al.*, 2001, 2005](#)). The most recent version, published in 2012 ([Barkovich *et al.*, 2012](#)), upholds the pivotal concept that MCDs derive from disruption of three major stages of cortical development: cell proliferation and apoptosis, cell migration, and post-migrational development. In particular, MCDs have been classified into these three main groups based on the main developmental stage that is first affected, acknowledging the fact that alteration of early developmental events often affects later events ([Barkovich *et al.*, 2012](#)). Moreover, these different processes take place at different times in different parts of the brain, so many different processes are often taking place simultaneously ([Barkovich *et al.*, 2012; Barkovich, 2013](#)).

The proliferation of neurons in the dorsal telencephalon of the human foetus begins around the fifth to sixth gestational week, decreases after 16 gestational weeks, and finishes around 22–25 gestational weeks ([Bystron *et al.*, 2008](#)). During the cell proliferation and apoptosis stage, pyramidal neuronal and glial precursors are generated from neuroepithelial cells in the ventricular zone (VZ), immediately adjacent to the lateral ventricle. The neuroepithelial cell population divides symmetrically and undergoes a stereotyped interkinetic nuclear migration (i.e. a process where the position of the cell nucleus is altered in line with the cell cycle), thus forming a pseudostratified monolayer ([Astick and Vanderhaeghen 2018; Borrell, 2019](#)). Following pool expansion, neuroepithelial cells will convert to apical radial

glial cells (aRGC), characterized by a unique epithelial morphology, partial glial identity, and high neurogenic capacity. In particular, aRGC divide at the ventricular surface either symmetrically, to produce two progenitors, or asymmetrically, generating a progenitor and a neuron, either directly or indirectly via intermediate progenitors ([Astick and Vanderhaeghen, 2018; Borrell 2019](#)). Intermediate progenitors are a specific class of progenitor cells without epithelial polarity that divide in the subventricular zone (SVZ) before generating neurons. Of note, aRGC span the entire cerebrum from the ependyma to the pia with their basal and apical processes, thus functioning as a stable radial scaffold for neuronal migration ([Bystron *et al.*, 2008](#)). At later stages of cortical neurogenesis, the proliferative compartment expands basally into a so-called outer SVZ that is much larger than the VZ ([Smart, 1973; Dehay *et al.*, 2015; Astick and Vanderhaeghen, 2018](#)). In particular, the outer SVZ contains specialized basal progenitors, the outer radial glia cells (oRGC), displaying a distinctive morphology (i.e. a basal process but not an apical process), a specific gene expression profile, and a specific and stereotyped movement at mitosis, known as mitotic somal translocation. Because of its strong proliferative capacities, the outer SVZ is extremely important in the development of primate/human cortex, likely contributing to its expansion as well as gyrification ([Lui *et al.*, 2011; Astick and Vanderhaeghen, 2018; Borrell, 2019](#)). Of note, the wide diversity of neurons that populate the cortex is mainly achieved by a mechanism of temporal patterning, in which cortical progenitors display a sequential shift in competence for the generation of different neuronal subtypes: early born excitatory neurons will occupy deep layers of the cortex, while late born neurons will migrate through these neurons to settle in the upper or superficial cortical layers, displaying specific and diverse laminar identities as well as typical morphological and functional features ([Astick and Vanderhaeghen, 2018](#)). Conversely, cortical inhibitory interneurons are generated in a separate ventral telencephalic niche, the medial and caudal ganglionic eminences, and, as explained below, they will undertake different migration trajectories to the dorsal telencephalon where they will integrate into cortical circuits ([Chu and Anderson, 2015; Astick and Vanderhaeghen, 2018](#)).

In cases of reduced proliferation or increased apoptosis, microcephaly may result; on the other hand, enhanced proliferation or reduced apoptosis can cause megalencephaly. Abnormal proliferation (also called dysgenesis) may also occur, resulting in dysmorphic neurons typical of type II focal cortical dysplasia (FCD) and megalencephaly with cortical malformations. These conditions have been recently recognized to result from germline and somatic mutations activating the mTOR pathway in dorsal telencephalic progenitors of excitatory neurons.

In the human cerebrum, migration of neurons begins at a time when the first neurons are formed (around fifth to sixth gestational week), peaks between the third and fifth months of gestation, and ends around 30–35 gestational weeks (cerebellar migration continues into the middle of the second

year of life) (Bystron *et al.*, 2008). The postmitotic neurons that have been generated must then find their final place of destination. They obtain bipolar morphology and migrate largely orthogonal to the brain surface guided by aRGC (Métin *et al.*, 2007). So, only after completing the last cell division and establishing their polarity, neurons begin to migrate from the VZ/SVZ. There are two modes of neuronal migration, as recently reviewed by Silva *et al.* (2019). The first and the most common one is radial migration, in which neurons initially migrate from one aRGC to another (from VZ to SVZ) and then they migrate parallel to the same aRGC (from SVZ to cortex), changing their morphology from an elongated, ‘bipolar’ to a ‘multipolar’ shape when entering the intermediate zone (Reillo *et al.*, 2011; Cooper, 2014; Pollen *et al.*, 2015). Several genes seem to directly regulate the transport of maturing neurons to the cortex through local production of growth factors, potentiation of growth factor signals by extracellular matrix proteins, and activation of self-renewal pathways (Cooper, 2014). The second mode of migration is tangential migration (i.e. orthogonal to aRGC), which is the mode of migration for most of the interneurons; the mechanism of this migration is not yet fully established (Tanaka and Nakajima, 2012; Chu and Anderson, 2015). Disorders of neuronal migration ensue when migration terminates too early or too late. Incomplete migration of neurons may be due to disruption of the neuroependyma, possibly because of abnormal vesicular trafficking, resulting in ‘gaps’ in the ependymal membrane and altered neuroependymal attachment of the aRGC (Lian and Sheen, 2015); neurons produced in the VZ that are not connected to the aRGC are unable to migrate, thus remaining at or near the ventricular border in the form of clusters of neurons recognized as periventricular nodular heterotopia. Alternatively, interrupted neuronal migration may be due to disruption of the complex molecular apparatus needed for moving neurons from the SVZ to the cortex, including tubulins, microtubule-associated proteins (such as LIS1 and DCX), and actins (Di Donato *et al.*, 2018). Mutations of genes regulating these processes result in a variable spectrum of MCD, including lissencephaly, microcephaly with lissencephaly and dysgyria (Di Donato *et al.*, 2017). Conversely, cortical over-migration into the leptomeninges may be due to defects in the pial surface of the brain and may result in a variable imaging spectrum of polymicrogyria/cobblestone malformations, as noted in dystroglycanopathies (Nakano *et al.*, 1996; Saito *et al.*, 1999), laminopathies (Vigliano *et al.*, 2009; Radner *et al.*, 2013), GPR56-related diseases (Li *et al.*, 2008; Vandervore *et al.*, 2017) or even acquired injuries (ischaemic, teratogenic or infectious). One hypothesis is that depending upon the size of the defects in this membrane, the resulting cortex may present a polymicrogyric (small gaps) or cobblestone appearance (large gaps) (Barkovich *et al.*, 2015; Desikan and Barkovich, 2016). In general, it is important to note that disturbance in the formation of the leptomeninges or loss of their normal signalling functions are potent contributors to cortical malformation.

The last step of cortical formation, called post-migrational development, is characterized by axonogenesis, dendritogenesis as well as synapse initiation, maturation and pruning involving both pyramidal neurons and cortical interneurons (Budday *et al.*, 2015; Chu and Anderson, 2015). These processes are intimately related to progressive cortical folding with formation of gyri and sulci that follow a specific, timely predictive pattern that may be assessed on foetal MRI (Budday *et al.*, 2015). Most post-migrational processes extend beyond the intrauterine period and some of them continue even into adult life (Budday *et al.*, 2015; Fernández *et al.*, 2016).

Isolated disorders of post-migrational development mainly include secondary microcephaly, FCD type I (Barkovich *et al.*, 2012) and certain forms of dysgyria. Although polymicrogyria is still classified as a post-migrational disorder (Barkovich *et al.*, 2012), there is increasing evidence that this malformation is mainly the consequence of disturbed late neuronal migration. Indeed, besides disruption of cortical organization with or without fusion of the overlying molecular layer, recent histopathology studies have shown that polymicrogyria is frequently characterized by defects in the pial limiting membrane and overlying meninges with associated leptomeningeal heterotopia (Squier and Jansen, 2014; Jansen *et al.*, 2016). These findings suggest the reclassification of polymicrogyria in the group of late migrational, rather than post-migrational, abnormalities. As cortical development remains a dynamic process well into postnatal life, it is likely that there are a vast number of disorders of cortical development of varying aetiologies that may not be detected using imaging. These disorders may impact on both grey and white matter development.

Current limits and open questions about classification

Classifications are not rigid, unmodifiable paradigms; rather, they should be viewed as dynamic, ‘fluid’ models that continuously evolve as knowledge is gained about underlying pathological mechanisms. The discovery of many genes, proteins, and pathways involved in cortical development has improved our understanding of MCD, making the classification schemes more complex in some areas and more simplified in others (Supplementary Table 1). Indeed, classification schemes are often challenged by the discovery of underlying genetic defects, since genotype-phenotype studies have demonstrated that different mutations in the same gene may lead to different types of MCD and mutations in different genes that function in the same pathway may cause the same cortical malformative pattern (Manzini and Walsh, 2011; Barkovich, 2013). Moreover, different pathological mechanisms may cause the same phenotypic MCD on imaging (Manzini and Walsh, 2011; Barkovich, 2013). Of note, all these data demonstrate the central role of common signalling

pathways and support the hypotheses that MCD-related genes are involved at multiple developmental stages and that proliferation, migration and post-migrational organization are genetically and functionally interdependent (Barkovich, 2013). As the boundaries between disorders of neuronal migration, cortical organization and proliferation are vanishing, it is expected that future classifications of MCDs will rely on the precise knowledge of those biological pathways (Barkovich, 2013; Guerrini and Dobyns, 2014).

How to study malformations of cortical development

Malformations of cortical development due to under- or over-migration are difficult to recognize by foetal ultrasound and MRI before 20 weeks of gestational age (in many countries an important time point for possible termination of pregnancy). Even after that date, identification remains a challenge. Abnormal sulcation patterns can be identified by ultrasound and/or MRI, either in the form of lack of normal sulci (consistent with the lissencephaly spectrum) and/or early, aberrant sulcation (consistent with polymicrogyria). While megalencephaly and microcephaly can be confidently assessed through measurements of the head circumference and—in the case of some megalencephalies—asymmetries in cerebral hemisphere volume, other subtler abnormalities such as grey matter heterotopia often remain altogether invisible. In all cases of suspected MCD on prenatal studies, post-natal confirmation with ultrasound and MRI should be obtained to delineate the abnormalities and their extension.

In the postnatal period, ultrasound can be used to look for calcification, disturbances of gyral architecture, enlarged ventricles, and midline defects, which could be direct or indirect signs of brain malformations. Malformations involving the posterior fossa are more difficult to detect, and should be imaged not only through the anterior fontanel but also through the mastoid fontanel (asterion). For optimal imaging, dedicated neonatal convex and high frequency linear transducers should be used. Proper training is of utmost importance for neonatal ultrasound as the technique is heavily operator dependent.

Although CT scanning can be used to study MCD and will depict most abnormalities with good detail, its routine use is discouraged in view of radioprotection concerns. CT is presently mostly used as a second-line imaging method to confirm calcifications that sometimes accompany brain malformations (such as those found in congenital cytomegalovirus infection), although the latter can often be confidently detected on MRI using susceptibility-weighted imaging (SWI).

MRI is certainly recommended as the most important imaging method in the evaluation of MCD, thanks to its optimal delineation of grey and white matter structures in the absence of ionizing radiation. Radiologists should strive to

maximize the quality of their MRI protocols when suspecting MCD, using the best/highest resolution/highest contrast scanner available in their institutions (Martinez-Rios *et al.*, 2016). We support the use of 3 T over 1.5 T scanners whenever available, provided that imaging protocols are optimized. Radiologists should also obtain detailed information from the referring clinicians regarding the size of the head, possible syndromic clinical features, epilepsy semiology, and EEG findings (particularly, location of origin of spikes) before reporting the examination (Martinez-Rios *et al.*, 2016).

Furthermore, it is of great importance to become familiar with the changes in imaging appearance of MCD associated with the age of the patient (Eltze *et al.*, 2005) and the type of magnetic resonance sequences that are best suited to detect these anomalies (Martinez-Rios *et al.*, 2016). Remarkably, ongoing myelination and maturation modifies the appearance of the normal grey and white matter and causes interval changes in the delineation of grey-white matter interfaces that, in turn, cause MCDs to become more or less easily identifiable at any given age. Specifically (i) contrast between cortex and white matter is maximal before myelination begins; (ii) during myelination, such contrast transiently diminishes; (iii) a ‘T₂ isointense’ stage is usually presented at 8–12 months, which may hinder recognition of MCDs; and (iv) during myelination, cortical thickness progressively increases. Such physiological modifications are particularly relevant in that, unless a malformation has been suspected prenatally and imaged for confirmation in the neonatal period, several patients with MCDs will present with psychomotor delay and/or seizures in the first year of life, and will therefore be first imaged in the T₂ isointense period. For these cases, repeat MRI after completion of myelination (i.e. in the third year of life) may be warranted to fully elucidate the picture.

The MRI protocol should reflect this dynamic context and be, therefore, adjusted with patient age. In the fully-myelinated brain, at least a thin slice (≤ 1 mm) 3D T₁-weighted sequence, axial and coronal T₂-weighted sequences (≤ 3 mm) and a FLAIR T₂ sequence (preferably 3D with thin slices, ≤ 1 mm, for triplanar reformatting) should be obtained. In newborns, however, T₂-weighted sequences obtained in the three planes of space are of paramount importance, whereas high-resolution T₁ 3D sequences can be more technically challenging and FLAIR is unnecessary (since incomplete myelination generates suboptimal grey-white matter contrast). In all cases, diffusion-tensor imaging is extremely important to inspect the microscopic architecture of the brain and to identify possible associated axonal pathfinding disorders, and should always be obtained at least in research contexts. A practical schematic approach for making the diagnosis of MCD on imaging is proposed in [Supplementary Fig. 1](#) and [Supplementary Table 2](#).

In case of a suspicion of MCD causing epilepsy, radiologists should also consider using nuclear medicine techniques, such as FDG PET, especially in MRI negative scans. Indeed,

interictal FDG PET coregistered to structural MRIs may aid in localizing epileptogenic MCD in surgical workup because of its hypometabolic appearance (Jayalakshmi *et al.*, 2019). If this still give equivocal results, an ictal SPECT can be performed to help to identify the epileptic zone by showing hyperperfusion. In the peri-ictal stage, perfusion MRI with arterial spin labelling (ASL) is also showing great promise in the identification of regional hyperperfusion secondary to the increased metabolic demands (Takahara *et al.*, 2018).

Normal cortical imaging

The fundamental ontologies of the cerebral cortex in mammals are the archicortex (represented by the hippocampal formation and related structures), the paleocortex (including the olfactory cortex), the periallocortex (consisting of the presubiculum, parasubiculum and entorhinal cortex) and the significantly larger neocortex or isocortex (Insausti *et al.*, 2017).

The normal human neocortex occupies ~90% of the overall cerebral cortical surface and consists of a compact, mostly six-layered, ribbon of grey matter (Raybaud and Widjaja, 2011; Insausti *et al.*, 2017). Although previous pathology studies reported that normal cortical thickness ranges from 1 to 4.5 mm (being thinner in the depth of the sulci and thicker at the crown of the gyri) (Fischl and Dale, 2000; Raybaud and Widjaja, 2011), cortical measurements using brain MRI should not be used as strict cut-off values in the assessment of MCD. Indeed, neocortical thickness on neuroimaging studies is known to vary with age, myelination status, gender, head size, and brain cortical area as well as secondary phenomena, such as acquired lesions or seizures (Raznahan *et al.*, 2012; Tang *et al.*, 2019).

In newborns and infants up to 6 months of age, the cortex is hypointense on T₂- and hyperintense on T₁-weighted MRI relative to the unmyelinated white matter ('infantile pattern') (Barkovich, 2000a; Paus *et al.*, 2001). Only after 1 year of age does an early adult pattern appear, first on T₁- and later on T₂-weighted images (Barkovich, 2000a; Paus *et al.*, 2001). The cortical-subcortical interface is well demarcated in the neonatal period but becomes more blurred in infants up to 1 year due to progression of myelination (Raybaud and Widjaja, 2011). This phenomenon is more striking between 8 and 12 months in the so-called 'isointense pattern' period (Paus *et al.*, 2001). Of note, FLAIR images before 2–3 years of age are even more difficult to assess because of incomplete myelination (Murakami *et al.*, 1999). As myelination progresses, at ~18 months the neocortex becomes hypointense on T₁-weighted MRI and hyperintense on T₂-weighted, FLAIR and diffusion-weighted (DWI) images when compared to the white matter. Notably, the embryologically older archi- and paleocortex are of subtly higher signal intensity on T₂, DWI, and FLAIR; these physiological regional signal variations can be observed in both healthy adults and children and are accentuated on 3 T MRI (Schneider and Vergesslich, 2007; Yeung *et al.*, 2013). This

finding is most probably explained by basic cytoarchitectural differences, as the paleocortex and archicortex have only three layers (Insausti *et al.*, 2017). In any case, the normal external cortical surface as well as the cortico-subcortical junction should always be smooth and sharply delineated (Raybaud and Widjaja, 2011). (Supplementary Fig. 2)

The normal human cortex is highly convoluted with up to two-thirds laying deep in the sulci (Raybaud and Widjaja, 2011). Importantly, any evaluation of the cortex should, therefore, always be accompanied by an analysis of the pattern of sulcation and gyration (Budday *et al.*, 2014). As a general rule, the primary and secondary sulci may show slight anatomical variations, but are constant and symmetric in location and depth (Raybaud and Widjaja, 2011) and are normally separated by <1.5 cm (Di Donato *et al.*, 2017).

Malformations of cortical development: definitions

Microcephaly

Microcephaly (or microcrania) refers to the clinical finding of a small head, with significant reduction in the occipital-frontal circumference (OFC) below –2 standard deviations (SD) (corresponding to the 3rd percentile) compared with age- and gender-matched controls (Ashwal *et al.*, 2009; Woods and Parker, 2013). An OFC comprising between –2 and –3 SD (corresponding to the 0.3 percentile) is considered mild microcephaly (Ashwal *et al.*, 2009). While microcephaly refers to a small head circumference, micrencephaly etymologically indicates a small volume of brain parenchyma. In practice, the growth arrest of the brain due to both acquired and genetic insults almost invariably results in a small head circumference (Raybaud and Widjaja, 2011). Therefore, in the vast majority of cases, microcephaly implies micrencephaly and the two terms have been used interchangeably. One exception are some craniosynostoses in which a small head circumference may be present despite normal brain size due to the early fusion of involved sutures.

Microcephaly is divided according to the time of occurrence into primary and secondary forms (Woods and Parker, 2013; Seltzer and Paciorkowski, 2014; Shaheen *et al.*, 2017). This basic distinction has proven useful to inform the diagnostic algorithm and prognosis of individual patients (Woods and Parker, 2013; Seltzer and Paciorkowski, 2014). Primary microcephaly, corresponding to previous 'microcephalia vera', is a congenital form of microcephaly often characterized by a simplified gyral pattern; it presents at birth or even *in utero* (Alcantara and ÓDriscoll, 2014; Seltzer and Paciorkowski, 2014; Naveed *et al.*, 2018). Most cases are believed to result from an impairment of the normal process of neurogenesis (Homem *et al.*, 2015) (including decreased progenitor pool size, number of cell cycles, ratio of proliferating cells to differentiating neurons, and abnormal or increased apoptotic events),

leading to a deficiency in the eventual number of neurons (Homem *et al.*, 2015); however, the underlying gene defect is only ascertained in only 59% of patients (von der Hagen *et al.*, 2014). In addition, since the volume of the neuropil is dependent upon the number of neurons present initially, the primary microcephalic head also tends to grow more slowly than normal (Herculano-Houzel *et al.*, 2007). Conversely, secondary microcephaly develops postnatally and is most commonly a consequence of disruptive events in the post-neurogenesis period (Seltzer and Paciorkowski, 2014). However, many individuals in this group present with an OFC in the lower normal range at birth. Based on the specific aetiopathogenetic mechanism, both primary and secondary microcephalies can be further classified into acquired/environmental or genetic (syndromic and non-syndromic) forms (Ashwal *et al.*, 2009).

Microcephaly may have normal or abnormal cortex and may be further classified based on the presence of associated cortical anomalies, such as simplified cortical gyral pattern, lissencephaly, grey matter heterotopia, and polymicrogyria (Fig. 1) (Vermeulen *et al.*, 2010; Adachi *et al.*, 2011). We define ‘simplified gyral pattern’ as a reduced number of gyri with shallow sulci (one-quarter to one-half of normal depth), but with normal thickness of the cerebral cortex on brain MRI (Fig. 1D–F). In the specific case of preterm or at term neonates with microcephaly, a delay of sulcation of at least 4 weeks could be considered abnormal. Of note, the degree of gyral pattern simplification is directly related to the severity of the microcephaly, and may have gradients of severity (Desir *et al.*, 2008). Conversely, in cases of microcephaly with lissencephaly (previously known as ‘microlissencephaly’), a simplified gyral pattern is associated with thickened cortex (Fig. 1G–O) (Barkovich *et al.*, 1998). It is currently well-established that microcephaly with lissencephaly does not correspond to a single entity, but rather to a heterogeneous group of disorders sharing similar neuroimaging features, often including severe cerebellar hypoplasia, with diverse underlying mechanisms (Di Donato *et al.*, 2018). Finally, microcephaly may be associated with polymicrogyria, which may have a unilateral or symmetric bilateral distribution, or with heterotopia (periventricular or subcortical nodules) due to acquired and genetic causes (see related paragraphs) (Fig. 1P–R).

Associated brain disorders, including other brain malformations (including basal ganglia, callosal, hind brain anomalies), white matter signal alterations or calcifications should be reported since the combination of some of these features may suggest specific aetiological diagnoses (Raybaud and Widjaja, 2011; Valence *et al.*, 2016).

Macrocephaly and brain overgrowth spectrum

Macrocephaly (or macrocrania) is a clinical term that refers to a generalized increase in size of the head, with an OFC exceeding the mean for age and gender by at least 2 SD (corresponding to the 97 percentile) (Boom, 2016). An OFC ranging between 2 and 3 SD (corresponding to the 99.7

percentile) above the mean is consistent with mild macrocephaly (DeMeyer, 1986). Megalencephaly differs from macrocephaly in that it refers to an increase in size of the brain. In contrast to the close relationship between microcephaly and micrencephaly, macrocephaly may be related to a wide variety of causes other than megalencephaly, including hydrocephalus, enlargement of extra-axial spaces and skeletal dysplasia (Mirzaa and Poduri, 2014; Keppler-Noreuil *et al.*, 2015; Winden *et al.*, 2015). Megalencephaly does not necessarily imply macrocrania, however, as brain overgrowth may be unilateral or even focal, thus not impacting significantly on head circumference (Mirzaa *et al.*, 2018). Megalencephaly may be caused by disruption of signalling pathways that regulate brain cellular proliferation, differentiation, cell cycle regulation, and survival (developmental megalencephaly) (Mirzaa and Poduri, 2014) or by some inborn errors of metabolism and leukodystrophies (metabolic megalencephaly) (Mirzaa and Poduri, 2014).

Although megalencephaly has been classically considered a single malformation, it is now recognized as a spectrum of brain overgrowth disorders (Mirzaa and Poduri, 2014; Mirzaa *et al.*, 2018). Brain overgrowth may be bilateral or unilateral, and in both cases either with complete or partial hemispheric involvement (Fig. 2 and Supplementary Fig. 3). Importantly, complete unilateral megalencephaly involving one or almost one entire brain hemisphere corresponds to the classical definition of hemimegalencephaly (HMEG) (Flores-Sarnat, 2002), while focal megalencephaly involving up to three cerebral lobes has been variably described as quadrantic dysplasia, lobar HMEG or hemi-HMEG (Fig. 2J–R); these are, in fact, mostly somatic mosaic mutations (see below) that usually involve predominantly the frontal lobe or the parieto-occipital lobes (D’Agostino *et al.*, 2004).

In HMEG the septum pellucidum and fornices are often thickened or deviated, with presence of mid-sagittal band-like structures connecting the frontal lobe with the limbic system, well seen on diffusion tensor imaging studies (Sato *et al.*, 2008). Moreover, all forms of megalencephaly (including HMEG) may either have normal-appearing cortex or be associated with cortical malformations (also known as dysplastic megalencephaly) and/or white matter signal abnormalities (Guerrini and Dobyns, 2014). Indeed, it was recently discovered that some dysplastic HMEG are merely large areas of focal cortical dysplasia type II (see following section), with the size of the area dependent upon both the timing and the extent of the causative mutation (D’Gama *et al.*, 2017).

Posterior cranial fossa structures may also be involved in the megalencephaly spectrum, although it is rather uncommon, with overgrowth of the cerebellum (with or without cerebellar cortical dysplasia) often progressing more rapidly than the cerebrum during the first 2 years of life, sometimes leading to acquired cerebellar tonsillar ectopia (Mirzaa *et al.*, 2012) (Fig. 2F and L). In the past, ‘total HMEG’ has been used to describe the specific association of HMEG with

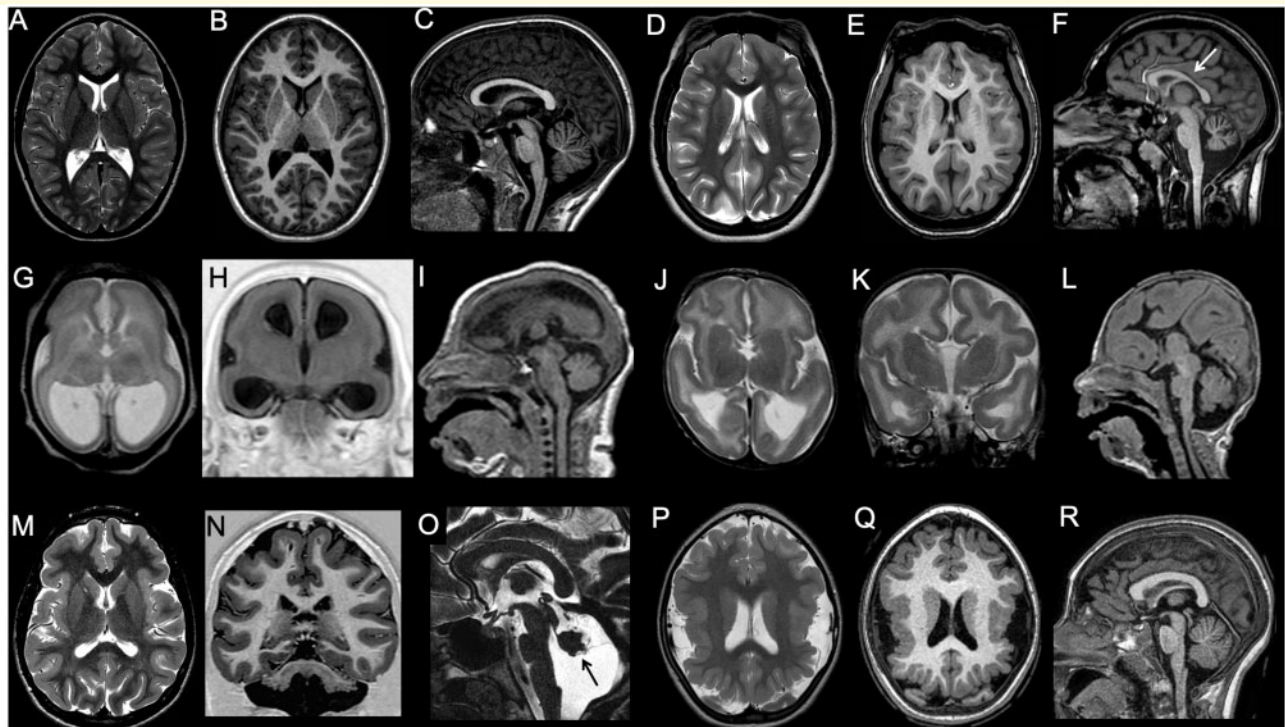


Figure 1 Imaging characteristics of microcephaly. (A–C) Microcephaly with normal gyration. In this 9-year-old male with head circumference (50 cm) below the third centile for age, gyrification is normal. Both corpus callosum and hindbrain are also well proportioned. (D–F) Microcephaly with simplified gyral pattern. The gyri are less numerous, and the sulci shallower and less deep than normal. Corpus callosum is also thin (arrow), and the vermis is mildly hypoplastic. (G–I) Microcephaly with lissencephaly. In this neonate, there is profound microcephaly with an almost complete absence of gyrification and thick cortex. There is concomitant ventriculomegaly, and pontine and corpus callosum hypoplasia (case courtesy of Zoltan Patay, USA). (J–L) Microcephaly with lissencephaly and agenesis of the corpus callosum. In this neonate, there is slightly less severe degree of microcephaly and simplified gyrification with thick cortex. There is associated pontine hypoplasia and corpus callosum agenesis (case courtesy of Zoltan Patay, USA). (M–O) Microcephaly with lissencephaly and midbrain-hindbrain involvement. In this patient with *VLDLR1* mutation, microcephaly is associated with gyral simplification and a thickened cortex. The corpus callosum is normal, and appears paradoxically larger. There is concomitant profound pontocerebellar hypoplasia, with prevalent vermis involvement (arrow). (P and R) Microcephaly with polymicrogyria. In this patient with *WDR62* mutation, microcephaly is associated with bilateral perisylvian polymicrogyria and with a simplified, aberrant gyral pattern in both parietal lobes. The corpus callosum and hindbrain are normal.

overgrowth of the ipsilateral brainstem and/or cerebellum (Sener, 1997). However, this term may be misleading since megalencephaly are frequently the result of a mosaic mutation (D’Gama *et al.*, 2017) and, therefore, the involvement of posterior cranial fossa is not confined to HMEG but it may be observed also in other megalencephaly forms (Guerrini and Dobyns, 2014).

Of note, megalencephaly with a variable range of cortical phenotypes, as seen on MRI, including polymicrogyria, can be isolated or a part of syndromic conditions, such as macrocephaly capillary malformation (MCM) and megalencephaly polymicrogyria-polydactyly hydrocephalus (MPPH) syndromes, epidermal naevus syndrome, congenital lipomatous asymmetric overgrowth of the trunk with vascular malformations, epidermal naevi, scoliosis/skeletal/spinal anomalies (CLOVES) syndrome, and other mTORopathies. These conditions are frequently associated with body overgrowth and cutaneous hallmarks, such as cutaneous naevi, due to neural crest involvement with the post-zygotic

somatic mosaicism (Mirzaa *et al.*, 2012; Keppler-Noreuil *et al.*, 2015).

Focal cortical dysplasia

The term ‘focal cortical dysplasia’ (FCD) refers to a spectrum of focal brain malformations characterized by disordered cortical lamination with or without abnormal cell types. In 2011, FCDs were categorized by the International League Against Epilepsy (ILAE) into three subgroups, essentially at pathology level (Blümcke *et al.*, 2011):

- (i) Type I (a–c) FCD are characterized by alterations in columnar/radial (Ia) or laminar/tangential (Ib) structure, or both (Ic) (Blümcke *et al.*, 2011). Type I FCD may affect small areas of the cortex and be difficult to detect even by an experienced neuropathologist. Because these cytoarchitectural aberrations may be subtle, type I FCD are often radiographically subtle or occult (Krssek *et al.*, 2008).

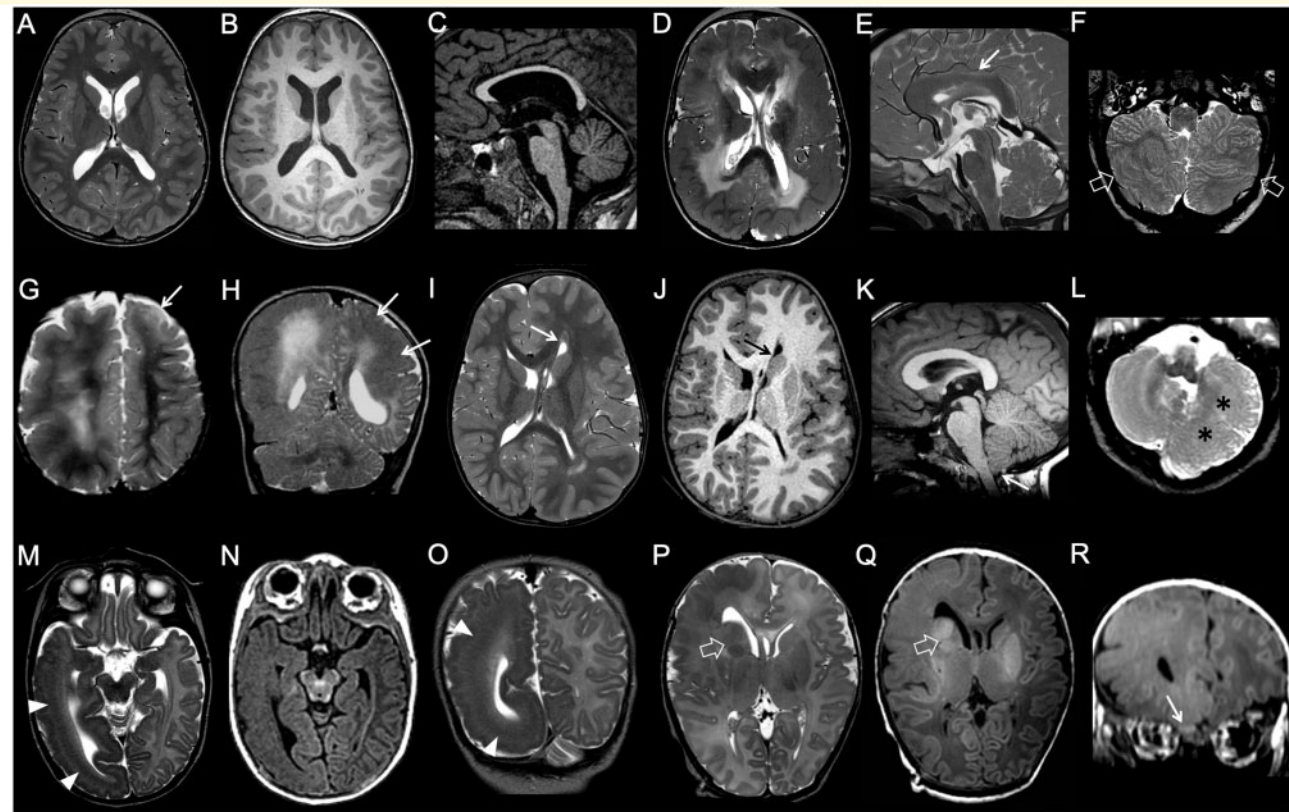


Figure 2 Imaging characteristics of megalencephaly. (A–C) Bilateral symmetrical brain overgrowth with normal-appearing cortex. Cortical thickness and convolitional patterns are normal, but global brain size is increased. The corpus callosum is thinned. (D–F) Bilateral symmetrical brain overgrowth with cortical malformations. There is a diffusely dysplastic cortex with an abnormal convolitional pattern, with a pachygyric appearance involving both hemispheres in an essentially symmetric distribution. Notice abnormal shape and orientation of frontal horns, related to aberrant septal bundles, and diffuse white matter signal abnormalities. The corpus callosum is thickened (arrow), and there is a diffusely dysplastic cerebellar cortex with grossly abnormal foliation (empty arrows). (G–H) Bilateral asymmetrical brain overgrowth with cortical malformations in two subjects. (G) Global enlargement of the right hemisphere with grossly abnormal, pachygyric cortex and hyperintense white matter is associated with more limited dysplasia of the left frontal pole (arrow). (H) Obvious right-sided megalencephaly is associated with left-sided pachygyria (arrows). (I–L) Unilateral complete brain overgrowth (also known as hemimegalencephaly). There is marked enlargement of one hemisphere with a dysplastic cortex and typical distortion of the ipsilateral frontal horn (arrows). Ipsilateral cerebellar hypertrophy is associated (asterisks). Note the mild tonsillar ectopia (arrow). (M–R) Unilateral partial brain overgrowth (also known as lobar hemimegalencephaly) in two neonates. (M–O) The enlargement is limited to the right temporo-occipital lobes, with evidence of subcortical band heterotopia (arrowheads). (P and R) There is marked enlargement of the right frontal lobe with abnormal gyral pattern and white matter signal. Note the enlarged right basal ganglia (empty arrows) and olfactory bulb (arrow) (case courtesy by Tamara Meulman, The Netherlands).

(ii) Type II (a, b) FCD are more often easily visualized by MRI (Krssek *et al.*, 2008) and are characterized by marked disruption of cortical lamination with presence of morphologically abnormal cell types, specifically dysmorphic neurons (characterized by abnormal shape, size, and orientation) and balloon cells (i.e. unusual large cells with abundant opalescent eosinophilic cytoplasm, one or more eccentric nuclei). Type IIa FCD has dysmorphic neurons only whilst type IIb FCD has both dysmorphic neurons and balloon cells (Blümcke *et al.*, 2011). Recent work has shown that type II FCD and dysplastic megalencephaly (including classical HMEG) form a spectrum of disorders that results from germline, somatic or germline plus somatic ‘two hit’ mutations of genes coding for proteins that function in the mTOR pathway (Jansen *et al.*, 2015; D’Gama *et al.*, 2017; Ribierre *et al.*, 2018).

(iii) Type III FCDs are essentially type I FCD with an additional brain lesion in the same lobe, and are classified as IIIa (hippocampal sclerosis), IIIb (tumour), IIIc (vascular malformation), or IIId (lesions acquired in early life, e.g. glial scar due to infectious or ischaemic injury) (Blümcke *et al.*, 2011). In contrast, if type II FCD are found in conjunction with, for example, hippocampal sclerosis or another structural lesion (such as vascular malformation or tumour), the two lesions are thought to reflect distinct pathological processes and termed ‘dual pathology’ or ‘double pathology’, respectively (Blümcke *et al.*, 2011).

Of note, a critical update of the international consensus classification of FCD by Najm *et al.* (2018) highlighting several challenges, especially regarding FCD types I and III, and

paving the way for a new integrated clinico-pathological and genetic classification system (Najm *et al.*, 2018; Blümcke, 2019). In particular, FCD type I subtypes are still lacking a comprehensive description of clinical phenotypes, reproducible imaging findings, and specific molecular/genetic biomarkers (Najm *et al.*, 2018). Moreover, molecular and clinical biomarkers are needed to differentiate between secondary (acquired) or primary aetiology of FCD III. Indeed, FCD adjacent to a non-developmental, postnatally acquired lesion is difficult to explain and FCD III might be not maintained as a separate entity in the upcoming revised classification (Najm *et al.*, 2018).

Regarding incidence of FCD, FCD IIa is the most common, followed by FCD IIb, FCD Ia, and FCD Ib; many authors believe that FCD IIa and IIb are closely related and a result of slightly different mechanisms. The tubers of the tuberous sclerosis complex (TSC) should be considered a subtype of FCDIIb because of the histological and imaging similarities, and shared aetiology due to involvement of the mTOR pathway genes *TSC1* and *TSC2*. The distinction between TSC and other form of FCDIIb lies in the accompanying clinical and imaging features necessary to fulfil diagnostic criteria for TSC (Northrup *et al.*, 2013). Associated imaging features often include subependymal nodules and giant cell astrocytoma which are both considered major diagnostic criteria for TSC in addition to the cortical tubers (Northrup *et al.*, 2013).

Relevant imaging findings of FCD include focal changes of cortical thickness, abnormal gyral and sulcal pattern, folds that are too large or too small, cortical and subcortical signal abnormalities (in one or all sequences), blurring of the grey-white matter junction, and a radially oriented and funnel-shaped high T₂/FLAIR signal intensity in the subcortical white matter pointing to the ipsilateral ventricle ('transmantle sign') (Fig. 3) (Krsek *et al.*, 2008; Raybaud and Widjaja, 2011; Colombo *et al.*, 2012). These features may be encountered individually or collectively and in variable associations (Colombo *et al.*, 2012). The transmantle sign is highly specific for FCD type IIb, including the tubers of TSC (Krsek *et al.*, 2008; Colombo *et al.*, 2012; Mellerio *et al.*, 2012). Another sign to look for on MRI is cortical swelling in the acute phase and later, presence of focal volume loss and/or reduced myelination caused by repeated seizures leading to tissue damage, best depicted on T₂ and FLAIR images (Krsek *et al.*, 2008; Raybaud and Widjaja, 2011). Finally, an asymmetric lack of subcortical myelination is a rather specific finding for FCD type Ia (Barkovich and Raybaud, 2019). Remarkably, the differential diagnosis includes low grade tumours, such as gangliogliomas, as well as new histological entities, such as 'oligodendrocytosis' (Mata-Mbemba *et al.*, 2018) and 'mild malformation of cortical development with oligodendroglial hyperplasia (MOGHE)' (Schurr *et al.*, 2017), characterized on MRI by abnormal signal intensities within the anatomical region of seizure onset.

Of note, imaging features may be very different in unmyelinated brains; in particular, during the neonatal phase FCD may have opposite signal characteristics on T₁ and T₂

images, often showing hypointense T₂ and hyperintense T₁ signal in the involved brain region (Baron and Barkovich, 1999) (Supplementary Fig. 4). This may be a very useful imaging finding at an age when the FCD itself may be difficult to identify (Eltze *et al.*, 2005). The explanation of this phenomenon is still uncertain, but several hypotheses have been proposed, including focal acceleration of the myelination processes as an attempt to repair or compensate for seizure-related tissue damage (Duprez *et al.*, 1998). Later, from 2 to 3 months until the end of the myelination process, FCD may be almost indistinguishable from the surrounding normal brain parenchyma, thus causing relevant false negative cases.

Not uncommonly, only very subtle changes (i.e. minimal blurring of cortex-white matter junction) or no clear abnormality can be seen on MRI in the regions corresponding to the epileptic focus, even in fully myelinated brains. Indeed, although magnetic resonance is useful for identifying most lesions, resection remains guided, in many cases, by abnormal cellular electrical activity detected by subdural or implanted parenchymal electrodes, or by hybrid imaging such as the combination of MRI and PET (Pestana Knight *et al.*, 2015).

Hypointense bands at the cortico-subcortical junction have been reported on susceptibility-weighted images obtained on 7 T magnetic resonance scanners (DeCiantis *et al.*, 2015). Calcification with type IIb FCD may also occasionally be seen, especially within the base of some tubers. This may be best appreciated on CT scanning. Finally, when FCD are clinically and electrically highly suspected, it is fundamental to review highly suspected areas of apparently normal MRI scans during or after multidisciplinary discussions, since many small and subtle FCD may be overlooked at a first (even careful) evaluation (Martinez-Rios *et al.*, 2016).

Grey matter heterotopia

Grey matter heterotopia are clusters of normal neurons in abnormal locations, mainly due to impaired migration (Aronica and Mühlebner, 2017). Heterotopia are identified on MRI in the form of conglomerates of grey matter in heterotopic locations and can be categorized based primarily on the morphology and location (Barkovich and Kuzniecky, 2000) (Fig. 4). Within each category, the pattern of distribution of grey matter heterotopia varies, but it may help to define the underlying genetic cause (Raybaud and Widjaja, 2011). Independently of the location, grey matter heterotopias are characteristically isointense with the cerebral cortex on all magnetic resonance pulse sequences (Barkovich and Kuzniecky, 2000).

Periventricular nodular heterotopia (previously designated as subependymal heterotopia) is the most common type, most often composed of nodules of grey matter lining the ventricular wall, varying widely in number, location, size, and (sometimes) shape variably associated with other brain or systemic malformations (Fig. 4A–D) (Barkovich and

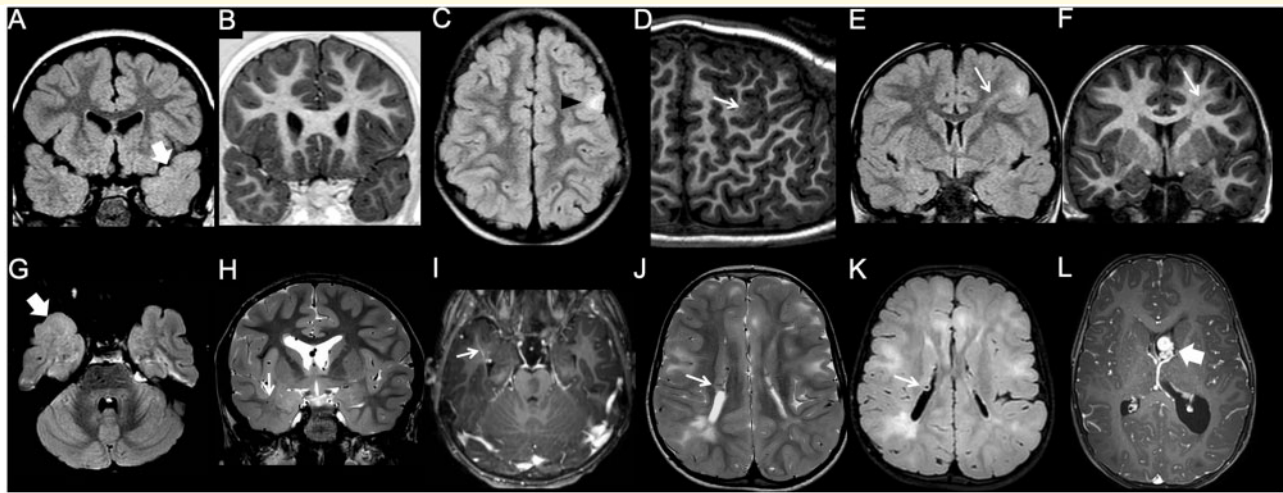


Figure 3 Imaging characteristics of focal cortical dysplasia. (A and B) Type I FCD. The left temporal pole is slightly smaller than the contralateral, and there is a blurred grey-white matter junction, with abnormal myelination compared to the contralateral side, best seen on the FLAIR image (arrow). (C and D) Type IIa FCD. There is focal, FLAIR-hyperintense cortico-subcortical lesion in the left frontal lobe (arrowhead). Curvilinear 3D T₁ reformat shows corresponding focal blurring of the grey-white matter junction (arrow). (E and F) Type IIb FCD. Focal cortico-subcortical area of hyperintensity in FLAIR, and hypointensity in T₁ is associated with typical transmantle sign (arrow). (G–I) Type III FCD. Slightly hypoplastic right temporal pole is associated with a blurred grey-white matter junction, better appreciated on the FLAIR image (thick arrow). Notice associated draining vein of a developmental venous anomaly (thin arrow). (J–L) Tuberous sclerosis complex. Typical, diffuse cortical tubers and white matter lesions are associated with subependymal nodules (thin arrows) and a subependymal giant cell astrocytoma arising at the left foramen of Monro (thick arrow).

Kuzniecky, 2000; Barkovich *et al.*, 2015). Periventricular nodular heterotopia should be differentiated from the subependymal nodules of tuberous sclerosis, which are not iso-intense with grey matter, often calcify, may enhance with contrast administration (when not calcified), and are oriented perpendicular to the ventricular walls (Barkovich and Kuzniecky, 2000; Barkovich *et al.*, 2015; Lu *et al.*, 2018). Rarely, periventricular heterotopia may appear as thick bands of heterotopic grey matter extending along the entire walls of the lateral ventricles (‘laminar heterotopia’) (Fig. 4E and F) (Mansour *et al.*, 2012). However, because of the resolution limitations of the magnetic resonance images of the reported patients, it is not clear yet if laminar heterotopia could be the result of confluent nodular grey matter heterotopias, or if it is a separate type of malformation characterized by smooth outer margins.

Subcortical heterotopia refers to collections of neurons dispersed in the white matter of the cerebral hemispheres (Barkovich, 2000b; Barkovich and Kuzniecky, 2000; Oegema *et al.*, 2019). Subcortical heterotopia has a broad imaging spectrum not totally covering its anatomical terminology. Indeed, heterotopia can be seen from the ventricle wall to the overlying cortex, but also in the deep white matter location (Raybaud and Widjaja, 2011). In the majority of cases, it extends from the ventricular surface to the overlying cortex, which is usually dysplastic, without well-defined intervening white matter (Fig. 4G and H) (Barkovich, 2000b; Barkovich and Kuzniecky, 2000). Such an arrangement is better-defined as ‘transmantle heterotopia’

composed of either thin bands of grey matter with a columnar morphology or larger masses with a bulkier appearance (Barkovich, 2000b; Barkovich and Kuzniecky, 2000; Barkovich *et al.*, 2012). In the latter subtype, the adjacent cortex (which is often malformed) appears continuous with the heterotopia, and the bulky masses form a curvilinear, swirling pattern due to a mixture of grey and white matter as well as engulfed blood vessels and CSF (Barkovich, 2000b; Barkovich and Kuzniecky, 2000; Barkovich *et al.*, 2012; Uccella *et al.*, 2019). The basal ganglia ipsilateral to bulky transmantle heterotopia may be small and dysmorphic (Barkovich, 2000b; Barkovich and Kuzniecky, 2000; Raybaud and Widjaja, 2011) with reduced white matter volume, probably as a result of a reduction of intrahemispheric associative fibres (Raybaud and Widjaja, 2011). Consequently, the affected hemisphere is frequently smaller than the contralateral (unaffected) one (Raybaud and Widjaja, 2011). Transmantle heterotopia sometimes involve one entire cerebral lobe, with a striking ‘lobe within a lobe’ appearance on imaging; this appearance has been called ‘sublobar dysplasia’ (Barkovich and Peacock, 1998; Barkovich *et al.*, 2012). A particular form of subcortical heterotopia characterized by giant, convoluted ribbons of heterotopic grey matter involving both cerebral hemispheres symmetrically and associated with corpus callosum agenesis and diffuse polymicrogyria, has been recently described (Kielar *et al.*, 2014); the term ‘ribbon-like heterotopia’ was proposed to describe this peculiar variant (Fig. 4M and N). Finally, very large midline ‘brain in brain’ malformations

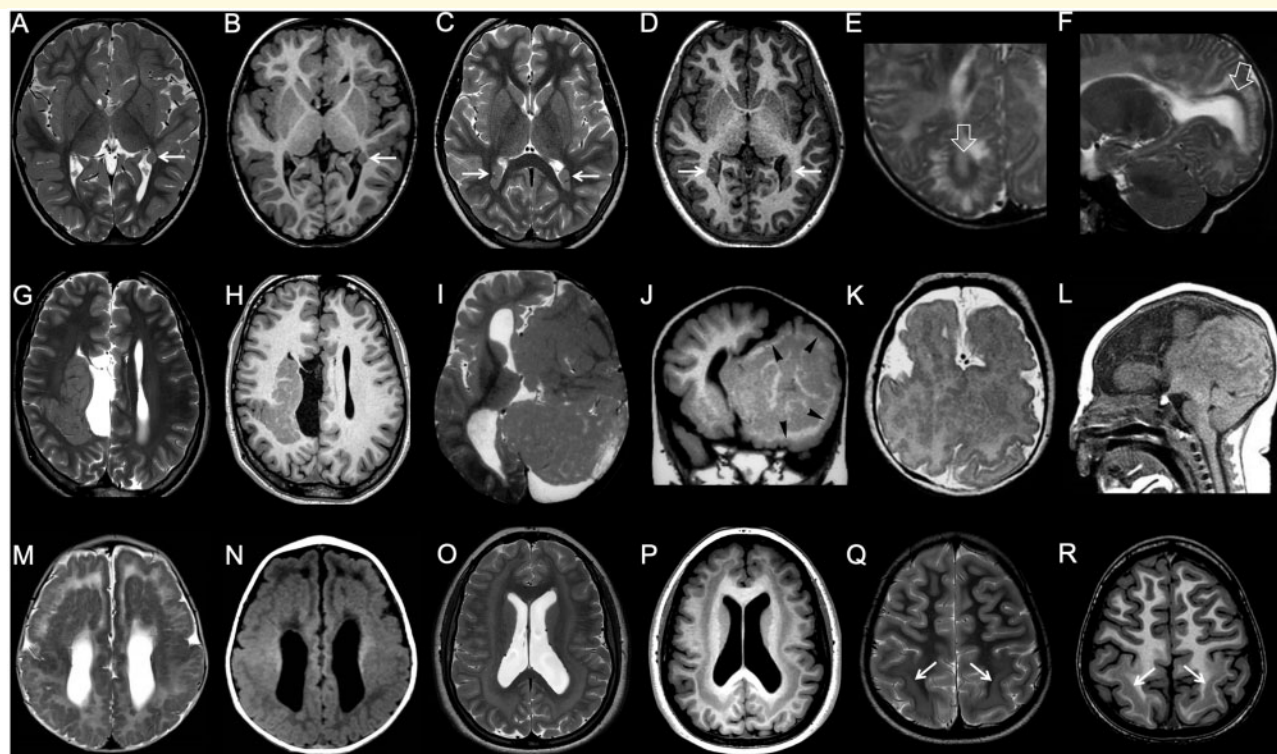


Figure 4 Imaging characteristics of grey matter heterotopia. (A and B) Single, unilateral periventricular nodular heterotopia. Single subependymal heterotopic nodule in the left paratrigenal region is isointense to grey matter on both T₁- and T₂-weighted images (arrow). (C and D) Multiple, bilateral periventricular nodular heterotopia. There are bilateral heterotopic nodules causing distortion of the bilateral trigonal margins (arrows). (E and F) Laminar heterotopia. There is a smooth, curvilinear heterotopic layer (arrows) associated with white matter abnormalities and overlying gyral simplification. (G and H) Subcortical, transmantle curvilinear heterotopia. In this patient with concurrent corpus callosum agenesis and a interhemispheric cyst, there is a large, convoluted grey matter heterotopia that curves across the whole thickness of right cerebral hemisphere. (I and J) Brain in brain malformation. Giant, gyriform heterotopia replaces most of left hemisphere. Overlying cortex is also abnormal (arrowheads) and there is concurrent corpus callosum agenesis. (K and L) Aventriculy. Grossly malformed, uncleaved telencephalon with extensive cortical malformation is associated with absence of the lateral and third ventricles (case courtesy of William B Dobyns, USA). (M and N) Diffuse band heterotopia. In this female with DCX mutation, grey matter heterotopia band extends across the white matter of both hemispheres in a symmetric fashion. Both outer and inner heterotopia margins are smooth. Overlying gyrification is simplified. (O and P) Posterior band heterotopia. Smooth-marginated heterotopia bands are present only in the parietal regions, in between normally myelinated white matter. Overlying gyrification is slightly simplified. (Q and R) Ribbon-like heterotopia. There is an undulated subcortical grey matter ribbon involving both hemispheres symmetrically. Overlying cortex is polymicrogyric, and there is corpus callosum agenesis. EML1 mutations have been recently described to cause this pattern (case courtesy of Jana Rydland, Norway).

with a bizarre mixture of grey and white matter have been described as variations of holoprosencephaly (Widjaja *et al.*, 2007); but we prefer to refer to these midline structures as ‘midline cerebral hamartomas’.

Subcortical band heterotopia (SBH) (previously called double cortex), is characterized by a smooth and poorly organized band of neurons which have arrested their migration in the subcortical or deep white matter, beneath the cortex proper (Barkovich *et al.*, 1989). SBH is currently considered part of the lissencephaly spectrum, based on the aetiological and genetic intersection between the two conditions (Dobyns, 2010). On MRI, SBH can be identified as a circumferential band of incompletely migrated, heterotopic grey matter deep to the cortical mantle, separated by well-defined, smoothly marginated layers of

normal-appearing white matter from both the overlying cerebral cortex and the underlying ventricle (Barkovich *et al.*, 1989). This band is usually bilateral and symmetrical and may be diffuse or partial. In the latter case, the band may be in a posterior or anterior location (Fig. 4O–R) (Di Donato *et al.*, 2017). Of note, in cases of partial SBH, the remaining cortex can be pachygyric (for instance anterior pachygyria with posterior SBH), possibly due to differential incomplete migration of neurons composing different cortical layers), and this should be carefully checked and reported. SBH can be also divided into thick (>7 mm) and thin (1–7 mm) subtypes (Di Donato *et al.*, 2017). Thick bands are usually located in the deep white matter beneath the deepest sulci (early cessation of migration), whereas thin bands tend to be located in the

subcortical white matter, adjacent to a gyrus (later cessation of migration) (Barkovich *et al.*, 1994). The overlying gyral pattern can be normal, but may have normal thickness with shallow sulci or can be frankly pachygyric.

Lissencephaly

Lissencephaly literally means ‘smooth head’ and is usually caused by impaired neuronal migration (Dobyns, 2010). The key features are a thickened cortex and a gyral abnormality ranging from agyria (absent gyration) to oligogyria (reduced gyration) (Dobyns, 2010; Di Donato *et al.*, 2017). The term agyria corresponds to a smooth brain with total absence of cortical convolutions (complete lissencephaly). Conversely, the term oligogyria is rarely used and is often substituted by ‘pachygyria’ (literally meaning ‘thick gyri’) to indicate a simplified convolitional pattern with few, broadened gyri and shallow sulci (Dobyns, 2010; Di Donato *et al.*, 2017). Complete agyria is extremely rare, seen most commonly in Miller-Dieker syndrome. Therefore, although it has been proposed that pachygyria can be distinguished from agyria based on the width of the involved gyri (Di Donato *et al.*, 2017), we suggest that the term agyria be uniquely used in the extremely rare cases where no sulci can be detected.

In the past, lissencephaly was categorized into two groups: lissencephaly type I, also known as classic lissencephaly, and lissencephaly type II, also known as cobblestone malformation (Dobyns *et al.*, 1985). It is now recognized that cobblestone malformation has a different pathophysiology than other forms of lissencephaly (i.e. over-migration instead of under-migration) and that the morphological appearance of the cortical surface is not smooth (Barkovich, 1996). Therefore, the cobblestone malformation was removed from the group of lissencephalies and the term lissencephaly type II has been discarded. Moreover, the differentiation of classic lissencephaly (lissencephaly type I), characterized by very thick cortex composed of two or four layers, and variant lissencephaly, characterized by mildly thickened cortex with three layers (Forman *et al.*, 2005), is no longer valid, in view of the advances of the genetic background pointing to different molecular mechanisms, which in turn determine the eventual cortical phenotype. Currently, lissencephaly is best classified based on the severity (grade) and gradient of the gyral malformation, cortical thickness, and presence of associated brain malformations (Di Donato *et al.*, 2018).

On imaging, the hallmark of lissencephaly is the presence of a thick cerebral cortex associated with reduced gyration (Fig. 5 and Supplementary Fig. 5) (Barkovich *et al.*, 1991; Landrieu *et al.*, 1998). In agyria, the most severe phenotype, the brain has a figure-of-eight shape resulting from a complete lack of sulci and wide, vertically oriented Sylvian fissures (Fig. 6A–C) (Dobyns, 2010). More often, at least a few shallow sulci are seen, subdividing the cortex into broad, coarse gyri, and leading to the morphological appearance of pachygyria (Dobyns, 2010). In general, lissencephaly is bilateral and symmetric,

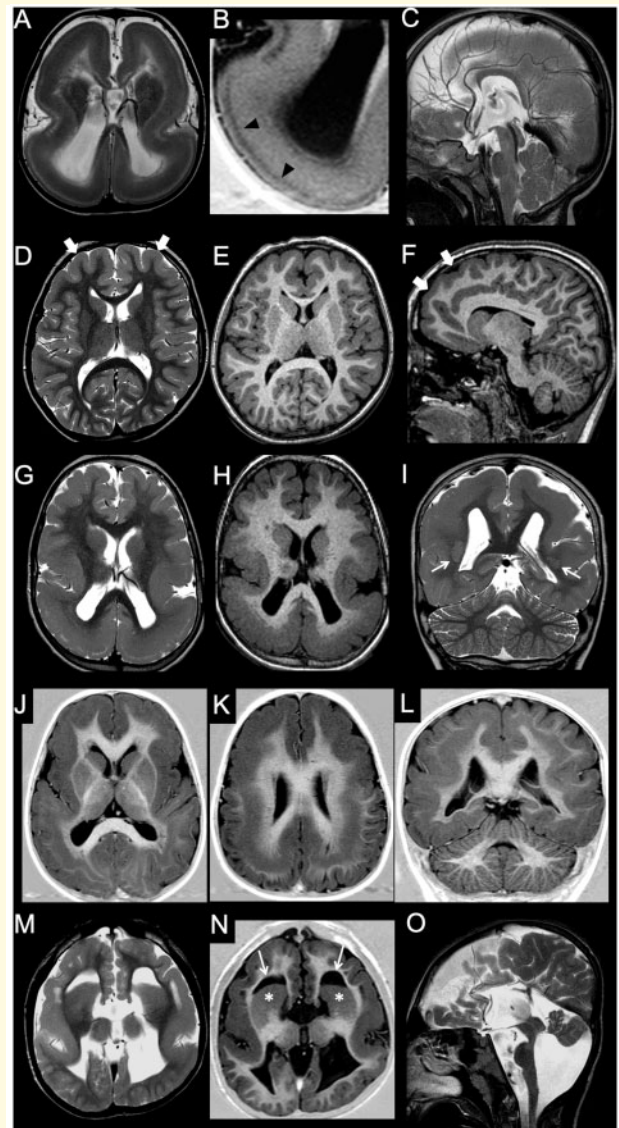


Figure 5 Imaging characteristics of lissencephaly. (A–C) Agyria. In this patient with a *LIS1* mutation there is complete absence of sulcation with a figure-of-eight appearance on axial images. Presence of a sparse cell layer zone (arrowheads) between thick arrested neuronal layer and thin superficial molecular layer. Note hypoplastic corpus callosum. (D–F) Pachygyria, frontal form. Gyration is somewhat simplified in the frontal lobes, with mild cortical thickening (arrows). (G–I) Pachygyria, posterior prevalence. In this patient with a *LIS1* mutation, there is almost complete agyria in the parietal lobes (with a sparse cell layer) and less severe pachygyria in the frontal lobes, establishing a typical postero-anterior gradient. Note grey matter heterotopia in the subcortical white matter (arrows). (J–L) Anterior pachygyria posterior double cortex. In this male patient with *DCX* mutation, there is frontal pachygyria associated with parietal SBH. Notice rudimentary convolutions overlying the heterotopic band. (M–O) In this patient with *TUBA1A* mutation there is bilateral perisylvian pachygyria associated with a less pronounced frontal pachygyria. Dysmorphic basal ganglia (asterisks) and frontal horns (arrows) that seem to wrap around the caudate heads are typical of tubulinopathies. There is associated vermian hypoplasia with a dysmorphic brainstem.

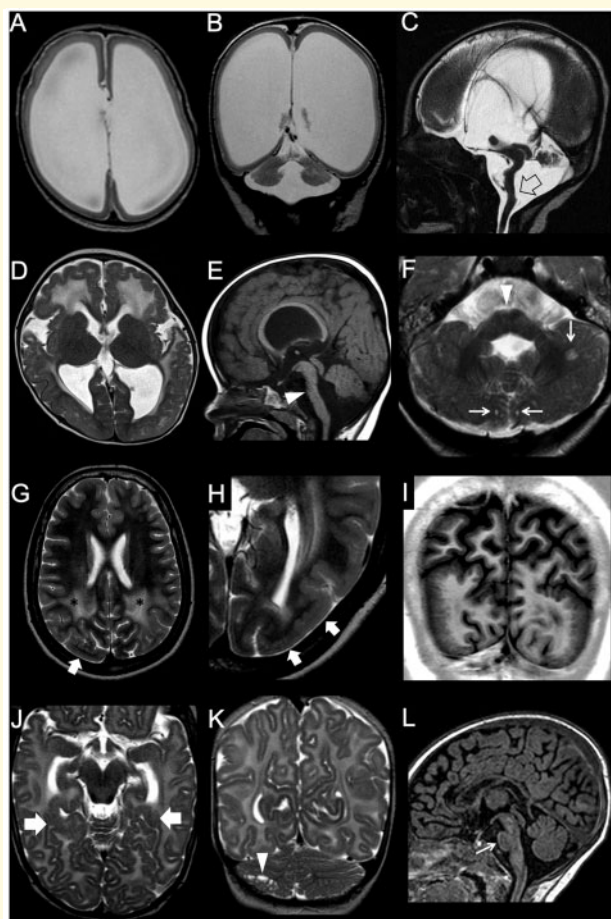


Figure 6 Imaging characteristics of cobblestone malformation. (A–C) Walker-Warburg phenotype. There is a severely thinned cerebral mantle with a complete lack of sulcation. The cortex is thin as most neurons have migrated in the subpial region. There is marked ventriculomegaly. Notice marked pontocerebellar hypoplasia with the characteristic brainstem kink (arrow) (case courtesy of Anna Nastro, Italy). (D–F) Muscle-eye-brain disease. Cobblestone pattern with a polymicrogyria-like appearance is associated with diffusely abnormal myelination and dysmorphic ventriculomegaly. Notice concurrent characteristic pontine cleft and cerebellar hypoplasia (arrowhead) with multiple microcysts (arrows) (case courtesy of Zoran Rumboldt, Croatia). (G–I) Posterior cobblestone in two subjects. (G–I) Cobblestone pattern involves both parietal lobes with a polymicrogyric appearance (arrows), with a flat surface and an irregular, lumpy-bumpy grey-white matter interface. Notice corresponding regional dysmyelination (asterisks). (J–L) In this patient with *LAMA2* mutation, there is a limited cobblestone cortex in the mesial temporo-occipital lobes (arrows) associated with cerebellar microcysts (arrowhead). Notice associated pontine hypoplasia (thin arrow).

usually involving the entire brain or large areas of the cerebral hemispheres with anterior or posterior predominance (Dobyns, 2010). The cortex is usually markedly thickened (10–20 mm), and referred to as ‘thick’ lissencephaly (Di Donato *et al.*, 2017), most often showing a four-layered structure; MRI can only resolve three layers,

however: the outer stripe corresponds to the molecular and outer cellular layers, the median stripe is characterized by T₁ and T₂ prolongation and corresponds to the cell-sparse layer, and the inner stripe is the thickest, corresponding to the inner layer of arrested neurons (Fig. 5B). In other instances, the cortex is less severely thickened (5–10 mm), and referred to as ‘thin’ lissencephaly (Di Donato *et al.*, 2017) (although it remains thicker than normal and thus the term ‘thin’ is in fact a misnomer). Alternatively, coexistence of areas of both ‘thick’ and ‘thin’ lissencephaly can be identified in the same patient, corresponding to ‘variable’ lissencephaly (Di Donato *et al.*, 2017). Of note, the subdivision of lissencephaly forms based on the thickness of the cortex, gradients of involvement and presence of other brain malformation is useful for predicting the most likely causative genes (Di Donato *et al.*, 2017).

On the milder side of the imaging and clinical spectrum of lissencephaly, one may find coexistence of both pachygyria and SBH (Fig. 5J–L) or isolated SBH with a normal or simplified gyral pattern of the overlying cortex (Dobyns, 2010). In association with all severities of lissencephaly, the grey-white matter junction is smooth and there may be a reduction of white matter volume, which correlates with the severity of the cortical malformation and consequently reduced thickness of the brain commissures and enlargement of the ventricular system (Raybaud and Widjaja, 2011). Moreover, cerebellar and basal ganglia malformations, callosal dysgenesis, and brainstem anomalies may be variably associated (Di Donato *et al.*, 2017).

The cobblestone malformation

The term ‘cobblestone malformation’ (previously known as type II lissencephaly or cobblestone lissencephaly) was initially proposed to define a rather specific cortical appearance characterized by irregular, pebbled external and internal surfaces resembling on MRI the morphology of a cobblestone (Barkovich, 1996). This cortical malformation is usually bilateral and symmetric, frequently involving the entire brain or large areas of the cerebral hemispheres with anterior (more frequently) or posterior predominance. It is caused by over-migration of neurons through ‘gaps’ (holes) in the pial limiting membrane that result from an inability of RGCs to attach to the pial limiting membrane (also called cortical pial basement membrane); as a result, neurons disengage from the radial glia, with some unable to reach the pial limiting membrane and others migrating through the ‘gaps’ into the subarachnoid space (Devisme *et al.*, 2012).

On imaging, cobblestone malformations are characterized by an undersulcated cerebral surface, with mildly to moderately thick cortex, and jagged cortical-white matter border with frequent vertical (perpendicular to the cortical-white matter border) striations (Fig. 7). This appearance is often highlighted by the presence of intracortical white matter high signal on T₂ and FLAIR. The underlying white matter may also show high signal, increasing the demarcation of

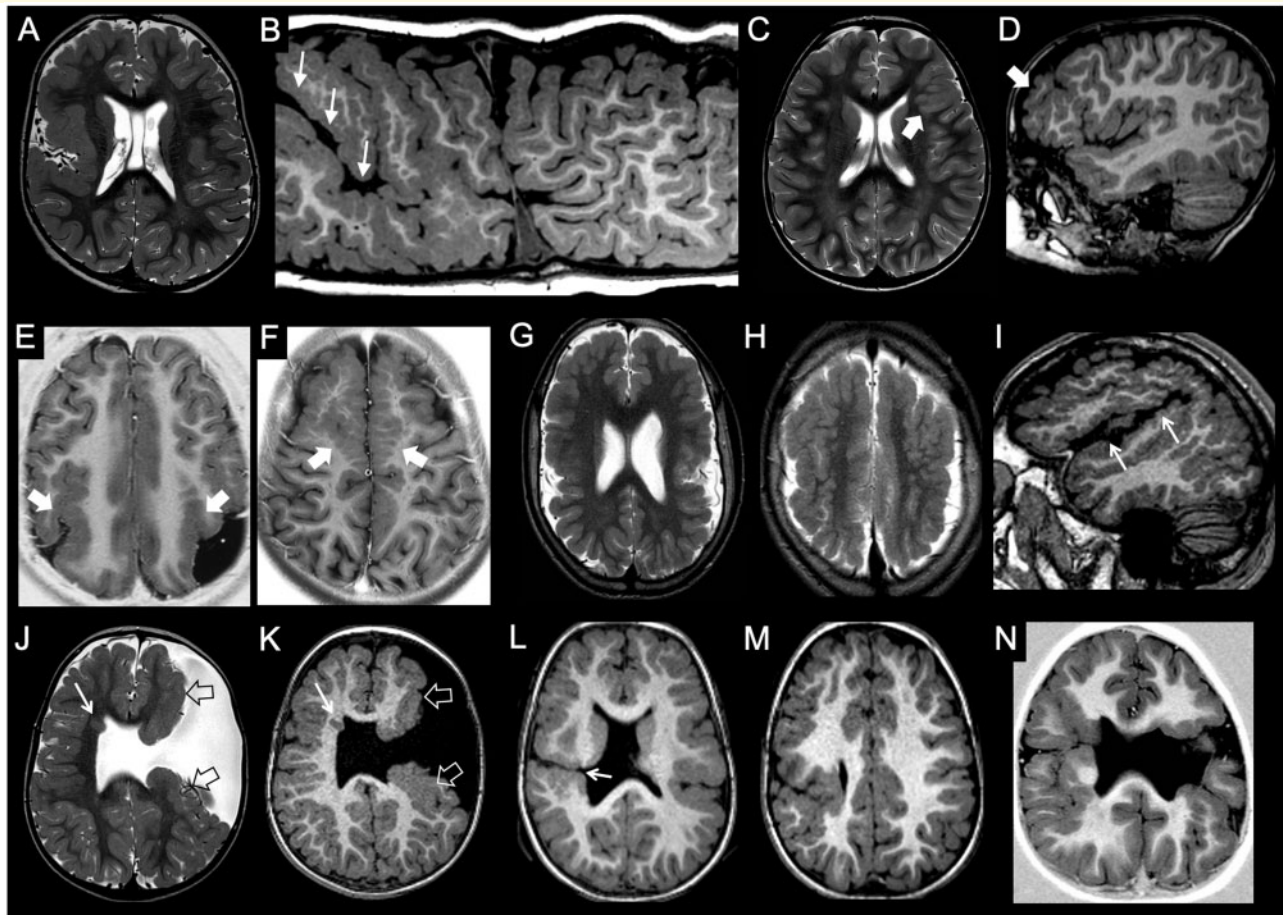


Figure 7 Imaging characteristics of polymicrogyria and schizencephaly. (A and B) Unilateral, diffuse polymicrogyria. There is unilateral perisylvian polymicrogyria, characterized by tightly packed microconvolutions and associated with anomalous orientation of the sylvian fissure (arrows). (C and D) Unilateral, focal polymicrogyria. There is a focal area with packed convolutions and abnormal gyration in the left frontal lobe (arrow). (E and F) Bilateral, regional polymicrogyria in two subjects. There is symmetric abnormal convolitional pattern involving the parietal (E, arrows) or frontal lobes (F, arrows), while the rest of the brain is unaffected. (G–I) Bilateral, diffuse polymicrogyria (fronto-parietal and perisylvian). There are multiple small convolutions diffusely involving the frontal and parietal lobes bilaterally, with abnormal orientation of the sylvian fissures (arrows). (J and K) Unilateral schizencephaly, open lips. There is a wide left transhemispheric cleft bordered by polymicrogyric cortex (open arrows). The septum pellucidum is absent, and there is contralateral periventricular heterotopia (arrow). (L and M) Unilateral schizencephaly, closed lips. There is a narrow right transhemispheric cleft bordered by polymicrogyric cortex. A dimple along the margin of the lateral ventricle signals the emergence of the cleft (arrow). The septum pellucidum is absent, and there is a concurrent contralateral polymicrogyric infolding. (N) Bilateral schizencephaly. There is right closed lips schizencephaly and left open lips schizencephaly associated with septal agenesis.

the cerebral cortical-white matter junction; however, these white matter signal abnormalities may be a temporary phenomenon that normalizes with age (Clement *et al.*, 2008; Barkovich *et al.*, 2015; Desikan and Barkovich, 2016; Brun *et al.*, 2017). There may also be characteristic posterior fossa abnormalities, such as brainstem clefts and cerebellar microcysts (postulated to be from extension of subarachnoid space through defects in the cerebellar pial limiting membrane) (Clement *et al.*, 2008; Barkovich *et al.*, 2015; Desikan and Barkovich, 2016). Of note, the cobblestone malformation includes several cortical phenotypes, ranging from an apparently undersulcated brain with relatively thin cortex, such as in the Walker-Warburg syndrome, to a more convoluted

and thicker cortex, such as in muscle-eye brain disease (Clement *et al.*, 2008; Barkovich *et al.*, 2015; Desikan and Barkovich, 2016).

Polymicrogyria

Polymicrogyria refers to an excessive number of abnormally small cerebral gyri (Stutterd and Leventer, 2014). In terms of anatomical distribution, polymicrogyria may be focal, multifocal, or generalized; it may be unilateral or bilateral; and it may be bilateral symmetric or bilateral asymmetric (Barkovich, 2010a; Stutterd and Leventer, 2014) (Fig. 7).

Polymicrogyria is a highly heterogeneous cortical malformation, being caused by both genetic and non-genetic causes, the latter including chromosomal abnormalities (such as 22q11 deletions and 1p36 monosomy) and single gene mutations (such as *COL4A1/COL4A2*, *OCN*, *RITN*, and *GRIN1* mutations) (Stutterd and Leventer, 2014). Of note, *in utero* infections (mainly by CMV or Zika virus), trauma, exposure to teratogens (including alcohol use), arterial ischaemic infarcts, twin-to-twin transfusion syndrome and death of a monozygotic twin are among the most frequent non-genetic causes of polymicrogyria (Raybaud and Widjaja, 2011). In these cases, an injury to the distal radial glia, pia or arachnoid has been demonstrated in foetal pathology specimens (Squier and Jansen, 2014). Alternative mechanisms for polymicrogyria include premature folding of the neuronal band, abnormal fusion of adjacent gyri, laminar necrosis of the developing cortex, and altered physical properties of the thickened leptomeninges exerting mechanical constraints on the developing cortex.

The most common location involves the Sylvian fissures (about 60–70% of cases), particularly the posterior aspect of the fissure (Fig. 7A and B); however, the polymicrogyria often spread beyond the immediate perisylvian region well into the frontal, parietal and temporal lobes, best seen on the parasagittal planes. Any part of the cerebral cortex including the frontal, occipital, and temporal lobes can be affected (Barkovich, 2010a; Leventer *et al.*, 2010; Stutterd and Leventer, 2014). When involving the perisylvian cortex, the Sylvian fissures are often abnormally extended posteriorly and superiorly and may show abnormal branching sulci lined by polymicrogyria (Fig. 7I).

Of note, polymicrogyria is descriptive term that designates a multiplicity of likely different entities with several appearances on imaging: thick and coarse, fine and delicate, with shallow or deep sulci (Barkovich, 2010b). Indeed, in polymicrogyria the cortical surface can have multiple small, delicate gyri, or it may appear thick and irregularly bumpy, with an appearance of ‘palisades’ of cortex, or it may be paradoxically smooth because the outer cortical (molecular) layer fuses over the microsulci (Barkovich, 2010b). Such variability most likely results from several factors, including technical MRI issues (amount of grey matter–white matter contrast, thickness of the slices), the stage of maturity/myelination of the brain at the time of imaging, and the type of polymicrogyria (Barkovich, 2010a). Remarkably, polymicrogyria may look different depending on the myelination stage (Supplementary Fig. 6), with a thin and bumpy or ‘stippled’ grey white junction best seen in the unmyelinated brain (2–3 mm) later evolving into an apparently thicker and relatively smooth cortex in the myelinated stage (5–8 mm) (Takanashi and Barkovich, 2003). Compared with lissencephaly the cortex is actually never truly thick, but is overfolded, yet may appear thickened on imaging. The underlying hypothesis in some cases is that a 4–5 mm layer of gliotic white matter runs through the polymicrogyric cortex, looking like white matter in the unmyelinated brain and like cortex after myelination (Takanashi and Barkovich, 2003).

The radiological spectrum of cobblestone malformation and polymicrogyria

It is important to remark that the imaging features of cobblestone malformation and polymicrogyria may partially overlap, potentially causing difficulties and discrepancies in their definition and classification. Accounting for this phenotypic variability, the concepts of ‘cobblestone/polymicrogyria-like’ cortex can be suggested in order to include this spectrum of appearances. In some polymicrogyria forms, these overlapping imaging features seems to be the result of shared pathophysiological mechanisms (Squier and Jansen, 2014; Jansen *et al.*, 2016). In particular, depending on the size of the gaps in the pial limiting membrane and the number of neurons migrating into the subarachnoid space, the resultant cortical phenotype may range from polymicrogyria (small gaps leading to small clumps of neurons on the cortical surface) to cobblestone malformation (large gaps leading to relatively smooth layers of neurons on the cortical surface) (Barkovich *et al.*, 2015; Desikan and Barkovich, 2016).

Of note, in severe cases of cobblestone malformation and polymicrogyria, the cortex appears thicker and is sometimes incorrectly described as ‘pachygyric’, despite the fact that classic lissencephaly (of which pachygyria is a subtype) has a completely different pathophysiological mechanism related to neuronal under-migration (Forman *et al.*, 2005), rather than over-migration. Remarkably, in these cases the apparently smooth surfaces on imaging may be due to technical limitations (i.e. insufficient spatial resolution) that may hamper the identification of irregularities of the cortical surface or cortical-white matter boundary (Raybaud and Widjaja, 2011).

Schizencephaly

Schizencephaly classically refers to a cleft lined by polymicrogyric grey matter and/or heterotopia extending across the full thickness of the cerebral hemispheres from the ventricular surface (ependyma) to the periphery (pial surface) of the brain as a ‘pial ependymal seam’ (Yakovlev and Wadsworth, 1946a, b; Byrd *et al.*, 1989). This malformation is probably the result of an early prenatal focal injury to the germinal matrix or, possibly, in infarct in very immature cerebrum with consequent liquefaction of injured tissue (Yakovlev and Wadsworth, 1946a). It is subdivided into open and closed lip forms depending on whether the cleft is fully patent and filled with CSF or, rather, sealed by the abutting cortical margins (Fig. 7J–N). In the latter form, a dimple along the ventricular margin signals the funnelled origin of the cleft (Barkovich and Kjos, 1992). On neuroimaging, differentiation of schizencephaly from purely clastic lesions, such as some types of porencephaly, is based on the fact that the schizencephalic cleft is lined by grey matter instead of white matter with variable grades of gliosis (Raybaud and Widjaja, 2011).

Schizencephalic clefts are frequently multiple and/or associated with contralateral polymicrogyria (Raybaud and Widjaja, 2011). In addition, abnormalities of the fornices and septum pellucidum frequently coexist, often as part of the ‘septo-optic dysplasia-plus’ spectrum (Griffiths, 2018).

Dysgyria

Dysgyria is a recently introduced term referring to a non-specific malformation in which the cortex is dysmorphic (Mutch *et al.*, 2016); the mechanism(s) of dysgenesis are not understood. Imaging shows normal cortical thickness but an abnormal gyral pattern characterized by abnormalities of sulcal depth and orientation, with a smooth cortical surface and radially oriented sulci, or narrow gyri separated by abnormally deep or shallow sulci. These areas show an irregular orientation of sulci and an imaging appearance that is not typical for polymicrogyria, pachygyria or a simplified gyral pattern. Dysgyria may be a difficult diagnosis, and a more quantitative approach, for instance based on gyrification index, could help to improve the diagnosis of this condition.

Dysgyria was initially described in association with mutations in one of the many tubulin genes and dystroglycanopathies (Oegema *et al.*, 2015; Mutch *et al.*, 2016), but the full

range of disorders in which it is seen is not yet known. As previously mentioned, the primary and secondary sulci may present slight anatomic variations, but are constant and symmetric in location and depth (Raybaud and Widjaja, 2011); they are normally located less than 1.5 cm apart from one another (Di Donato *et al.*, 2017). Therefore, having considered the normal intra-individual and inter-individual variability, significant differences in the sulcation pattern on imaging may be considered consistent with dysgyria. Of note, there may be diffuse forms involving the entire brain as well as localized forms affecting specific and usually symmetrical brain regions (Fig. 8). Moreover, there may be primary forms due to genetic conditions such as *FGFR3* (Manikkam *et al.*, 2018) and *FGFR2* mutations (Stark *et al.*, 2015) as well as tubulin mutations (Oegema *et al.*, 2015; Mutch *et al.*, 2016; Romaniello *et al.*, 2018) (Fig. 8A–D), or secondary forms due to distortion of the sulcation pattern from presence or absence of nearby intracranial structures [such as in the case of stenogyria due to the absence of the cerebral falx in the Chiari II malformation (Miller *et al.*, 2008)], or in the case of *ACTA2* mutations where the rigidity of the abnormal arteries probably leads to an abnormal conformation of the mesial hemispheric sulci (D’Arco *et al.*, 2018) (Fig. 8E–H).

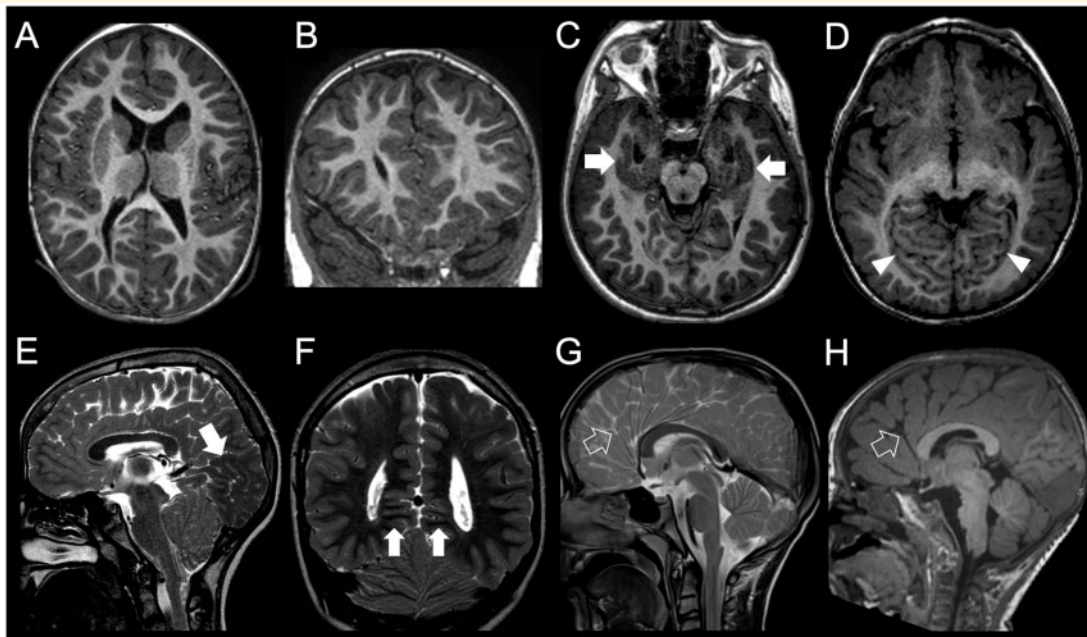


Figure 8 Imaging characteristics of dysgyria. (A and B) Primary diffuse dysgyria, bilateral, asymmetric form. The gyrification is bilaterally and asymmetrically abnormal, with an anomalous orientation of the sulci. The cortex, however, has normal thickness. (C and D) Primary focal dysgyria, bilateral, symmetric form, in two subjects. (C) In this patient with achondroplasia due to *FGFR3* mutation there is an abnormal orientation of the sulci along the inferomedial temporal lobes (arrows). (D) In this patient with Angelman syndrome there is abnormal orientation of the sulci in the occipital lobes (arrowheads). (E–H) Secondary dysgyria in three subjects. (E and F) In this patient with a Chiari II malformation there is crowding of the convolutions in the medial occipital and parietal lobes (arrows). The condition is known as ‘stenogyria’ and is not associated to cortical structural abnormalities. (G and H) In these two patients with *ACTA2* mutation, orientation of mesial sulci is abnormal secondary to arterial wall stiffness and straightening. Notice, in particular, absence of a clearly defined cingulate gyrus in both (empty arrows) (images courtesy of Felice D’Arco, UK).

Funding

This work was supported by the European Cooperation in Science and Technology (COST) Action CA16118 (<https://www.cost.eu/actions/CA16118/#tabs{Name:overview}>).

Competing interests

The authors report no competing interests.

Supplementary material

Supplementary material is available at *Brain* online.

References

- Adachi Y, Poduri A, Kawaguch A, Yoon G, Salih MA, Yamashita F, et al. Congenital microcephaly with a simplified gyral pattern: associated findings and their significance. *AJNR Am J Neuroradiol* 2011; 32: 1123–9.
- Alcantara D, ÓDriscoll M. Congenital microcephaly. *Am J Med Genet C Genet* 2014; 166C: 124–39.
- Aronica E, Mühlebner A. Neuropathology of epilepsy. *Handb Clin Neurol* 2017; 145: 193–216.
- Ashwal S, Michelson D, Plawner L, Dobyns WB. Quality Standards Subcommittee of the American Academy of Neurology and the Practice Committee of the Child Neurology Society. Practice parameter: evaluation of the child with microcephaly (an evidence-based review): report of the Quality Standards Subcommittee of the American Academy of Neurology and the Practice Committee of the Child Neurology Society. *Neurology* 2009; 73: 887–97.
- Astick M, Vanderhaeghen P. From human pluripotent stem cells to cortical circuits. *Curr Top Dev Biol* 2018; 129: 67–98.
- Barkovich AJ. Imaging of the cobblestone lissencephalies. *AJNR Am J Neuroradiol* 1996; 17: 615–8.
- Barkovich AJ. Concepts of myelin and myelination in neuroradiology. *AJNR Am J Neuroradiol* 2000a; 21: 1099–109.
- Barkovich AJ. Morphologic characteristics of subcortical heterotopia: MR imaging study. *AJNR Am J Neuroradiol* 2000b; 21: 290–5.
- Barkovich AJ. Current concepts of polymicrogyria. *Neuroradiology* 2010a; 52: 479–87.
- Barkovich AJ. MRI analysis of sulcation morphology in polymicrogyria. *Epilepsia* 2010b; 51: 17–22.
- Barkovich AJ, Dobyns WB, Guerrini R. Malformations of cortical development and epilepsy. *Cold Spring Harb Perspect Med* 2015; 5: a022392.
- Barkovich AJ, Ferriero DM, Barr RM, Gressens P, Dobyns WB, Truwit CL, et al. Microlissencephaly: a heterogeneous malformation of cortical development. *Neuropediatrics* 1998; 29: 113–9.
- Barkovich AJ, Guerrini R, Battaglia G, Kalifa G, N'Guyen T, Parmeggiani A, et al. Band heterotopia: correlation of outcome with magnetic resonance imaging parameters. *Ann Neurol* 1994; 36: 609–17.
- Barkovich AJ, Guerrini R, Kuzniecky RI, Jackson GD, Dobyns WB. A developmental and genetic classification for malformations of cortical development: update 2012. *Brain* 2012; 135: 1348–69.
- Barkovich AJ, Jackson DJ, Boyer RS. Band heterotopias: a newly recognized neuronal migration anomaly. *Radiology* 1989; 171: 455–8.
- Barkovich AJ, Kjos BO. Schizencephaly: correlation of clinical findings with MR characteristics. *AJNR Am J Neuroradiol* 1992; 13: 85–94.
- Barkovich AJ, Koch TK, Carrol CL. The spectrum of lissencephaly: report of ten patients analyzed by magnetic resonance imaging. *Ann Neurol* 1991; 30: 139–46.
- Barkovich AJ, Kuzniecky R, Jackson GD, Guerrini R, Dobyns WB. A developmental and genetic classification for malformations of malformations of cortical development. *Neurology* 2005; 65: 1873–87.
- Barkovich AJ, Kuzniecky RI. Gray matter heterotopia. *Neurology* 2000; 55: 1603–8.
- Barkovich AJ, Kuzniecky RI, Dobyns WB, Jackson GD, Becker LE, Evrard P. A classification scheme for malformations of cortical development. *Neuropediatrics* 1996; 27: 59–63.
- Barkovich AJ, Kuzniecky RI, Jackson GD, Guerrini R, Dobyns WB. Classification system for malformations of cortical development: update 2001. *Neurology* 2001; 57: 2168–78.
- Barkovich AJ, Peacock W. Sublobar dysplasia: a new malformation of cortical development. *Neurology* 1998; 50: 1383–7.
- Barkovich AJ, Raybaud C. Pediatric malformations of the brain and skull. In: AJ Barkovich, C Raybaud, editors. *Pediatric neuroimaging*. Philadelphia: Wolters-Kluwer; 2019. p. 405–632.
- Barkovich JA. Complication begets clarification in classification. *Brain* 2013; 136: 368–73.
- Baron Y, Barkovich AJ. MR imaging of tuberous sclerosis in neonates and young infants. *AJNR Am J Neuroradiol* 1999; 20: 907–16.
- Blümcke I. It is time to move on: commentary to: genotype-phenotype correlations in focal malformations of cortical development: a pathway to integrated pathological diagnosis in epilepsy surgery. *Brain Pathol* 2019; 29: 467–8.
- Blümcke I, Thom M, Aronica E, Armstrong DD, Vinters HV, Palmini A, et al. The clinicopathologic spectrum of focal cortical dysplasias: a consensus classification proposed by an ad hoc Task Force of the ILAE Diagnostic Methods Commission. *Epilepsia* 2011; 52: 158–74.
- Boom JA. Microcephaly in infants and children: Etiology and evaluation. [Internet] 2019 UpToDate; 2016. Available from <https://www.uptodate.com/contents/microcephaly-in-infants-and-children-etiology-and-evaluation> (May 2016, date last accessed).
- Borrell V. Recent advances in understanding neocortical development. *F1000Res* 2019; 8: 1791. (F1000 Faculty Rev)
- Brun BN, Mockler SRH, Laubscher KM, Stephan CM, Wallace AM, Collison JA, et al. Comparison of brain MRI findings with language and motor function in the dystroglycanopathies. *Neurology* 2017; 88: 623–9.
- Budday S, Raybaud C, Kuhl E. A mechanical model predicts morphological abnormalities in the developing human brain. *Sci Rep* 2014; 4: 5644.
- Budday S, Steinmann P, Kuhl E. Physical biology of human brain development. *Front Cell Neurosci* 2015; 9: 257.
- Byrd SE, Osborn RE, Bohan TP, Naidich TP. The CT and MR evaluation of migrational disorders of the brain. Part II. Schizencephaly, heterotopia and polymicrogyria. *Pediatr Radiol* 1989; 19: 219–22.
- Bystron I, Blakemore C, Rakic P. Development of the human cerebral cortex: boulder Committee revisited. *Nat Rev Neurosci* 2008; 9: 110–22.
- Chu J, Anderson SA. Development of cortical interneurons. *Neuropsychopharmacol* 2015; 40: 16–23.
- Clement E, Mercuri E, Godfrey C, Smith J, Robb S, Kinali M, et al. Brain involvement in muscular dystrophies with defective dystroglycan glycosylation. *Ann Neurol* 2008; 64: 573–82.
- Colombo N, Tassi L, Deleo F, Citterio A, Bramerio M, Mai R, et al. Focal cortical dysplasia type IIa and IIb: MRI aspects in 118 cases proven by histopathology. *Neuroradiology* 2012; 54: 1065–77.
- Cooper JA. Molecules and mechanisms that regulate multipolar migration in the intermediate zone. *Front Cell Neurosci* 2014; 8: 386.
- D'Agostino MD, Bastos A, Piras C, Bernasconi A, Grisar T, Tsur VG, et al. Posterior quadrantic dysplasia or hemi-hemimegalencephaly: a characteristic brain malformation. *Neurology* 2004; 62: 2214–20.
- D'Arco F, Alves CA, Raybaud C, Chong WKK, Ishak GE, Ramji S, et al. Expanding the distinctive neuroimaging phenotype of ACTA2 mutations. *AJNR Am J Neuroradiol* 2018; 39: 2126–31.
- D'Gama AM, Woodworth MB, Hossain AA, Bizzotto S, Hatem NE, LaCoursiere CM, et al. Somatic mutations activating the mTOR

- pathway in dorsal telencephalic progenitors cause a continuum of cortical dysplasias. *Cell Rep* 2017; 21: 3754–66.
- DeCiantis A, Barkovich AJ, Cosottini M, Barba C, Montanaro D, Costagli M, et al. Ultra-high-field MR imaging in polymicrogyria and epilepsy. *AJNR Am J Neuroradiol* 2015; 36: 309–16.
- Dehay C, Kennedy H, Kosik KS. The outer subventricular zone and primate-specific cortical complexification. *Neuron* 2015; 85: 683–94.
- DeMeyer W. Megalencephaly: types, clinical syndromes, and management. *Pediatr Neurol* 1986; 2: 321–8.
- Desikan RS, Barkovich AJ. Malformations of cortical development. *Ann Neurol* 2016; 80: 797–810.
- Desir J, Cassart M, David P, Van Bogaert P, Abramowicz M. Primary microcephaly with ASPM mutation shows simplified cortical gyration with antero-posterior gradient pre- and post-natally. *Am J Med Genet A* 2008; 146A: 1439–43.
- Devisme L, Bouchet C, Gonzalès M, Alanio E, Bazin A, Bessières B, et al. Cobblestone lissencephaly: neuropathological subtypes and correlations with genes of dystroglycanopathies. *Brain* 2012; 135: 469–82.
- Di Donato N, Chiari S, Mirzaa GM, Aldinger K, Parrini E, Olds C, et al. Lissencephaly: expanded imaging and clinical classification. *Am J Med Genet A* 2017; 173: 1473–88.
- Di Donato N, Timms AE, Aldinger KA, Mirzaa GM, Bennett JT, Collins S, et al. Analysis of 17 genes detects mutations in 81% of 811 patients with lissencephaly. *Genet Med* 2018; 20: 1354–64.
- Dobyns WB. The clinical patterns and molecular genetics of lissencephaly and subcortical band heterotopia. *Epilepsia* 2010; 51 (Suppl 1): 5–9.
- Dobyns WB, Kirkpatrick JB, Hittner HM, Roberts RM, Kretzer FL. Syndromes with lissencephaly. II: walker-Warburg and cerebro-oculo-muscular syndromes and a new syndrome with type II lissencephaly. *Am J Med Genet* 1985; 22: 157–95.
- Duprez T, Ghariani S, Grandin C, Smith AM, Gadisseux JF, Evrard P. Focal seizure-induced premature myelination: speculation from serial MRI. *Neuroradiology* 1998; 40: 580–2.
- Eltze CM, Chong WK, Bhate S, Harding B, Neville BGR, Cross JH. Taylor-type focal cortical dysplasia in Infants: some MRI lesions almost disappear with maturation of myelination. *Epilepsia* 2005; 46: 1988–92.
- Fernández V, Llinares-Benadero C, Borrell V. Cerebral cortex expansion and folding: what have we learned? *EMBO J* 2016; 35: 1021–44.
- Fischl B, Dale AM. Measuring the thickness of the human cerebral cortex from magnetic resonance images. *Proc Natl Acad Sci USA* 2000; 97: 11050–5.
- Flores-Sarnat L. Hemimegalencephaly: part 1. Genetic, clinical, and imaging aspects. *J Child Neurol* 2002; 17: 373–84.
- Forman MS, Squier W, Dobyns WB, Golden JA. Genotypically defined lissencephalies show distinct pathologies. *J Neuropathol Exp Neurol* 2005; 64: 847–57.
- Griffiths PD. Schizencephaly revisited. *Neuroradiology* 2018; 60: 945–60.
- Guerrini R, Dobyns WB. Malformations of cortical development: clinical features and genetic causes. *Lancet Neurol* 2014; 13: 710–26.
- von der Hagen M, Pivarcsi M, Liebe J, von Bernuth H, Di Donato N, Hennermann JB, et al. Diagnostic approach to microcephaly in childhood: a two-center study and review of the literature. *Dev Med Child Neurol* 2014; 56: 732–41.
- Herculano-Houzel S, Collins CE, Wong P, Kaas JH. Cellular scaling rules for primate brains. *Proc Natl Acad Sci USA* 2007; 104: 3562–7.
- Homem CCF, Repic M, Knoblich JA. Proliferation control in neural stem and progenitor cells. *Nat Rev Neurosci* 2015; 16: 647–59.
- Insausti R, Muñoz-López M, Insausti AM, Artacho-Pérula E. The human periallocortex: layer pattern in presubiculum, parasubiculum and entorhinal cortex. A review. *Front Neuroanat* 2017; 11: 84.
- Jansen AC, Robitaille Y, Honavar M, Mullatti N, Leventer RJ, Andermann E, et al. The histopathology of polymicrogyria: a series of 71 brain autopsy studies. *Dev Med Child Neurol* 2016; 58: 39–48.
- Jansen LA, Mirzaa GM, Ishak GE, ÓRoak BJ, Hiatt JB, Roden WH, et al. PI3K/AKT pathway mutations cause a spectrum of brain malformations from megalencephaly to focal cortical dysplasia. *Brain* 2015; 138: 1613–28.
- Jayalakshmi S, Nanda SK, Vooturi S, Vadapalli R, Sudhakar P, Madigubba S, et al. Focal cortical dysplasia and refractory epilepsy: role of multimodality imaging and outcome of surgery. *AJNR Am J Neuroradiol* 2019; 40: 892–8.
- Kepler-Noreuil KM, Rios JJ, Parker VER, Semple RK, Lindhurst MJ, Sapp JC, et al. PIK3CA-related overgrowth spectrum (PROS): diagnostic and testing eligibility criteria, differential diagnosis, and evaluation. *Am J Med Genet A* 2015; 167A: 287–95.
- Kielar M, Tuy FP, Bizzotto S, Lebrand C, de Juan Romero C, Poirier K, et al. Mutations in *Eml1* lead to ectopic progenitors and neuronal heterotopia in mouse and human. *Nat Neurosci* 2014; 17: 923–33.
- Klonowski W. Applications of chaos theory methods in clinical digital pathology. In: CH Skiadas, C Skiadas, editors. *Handbook of applications of chaos theory*. Boca Raton, FL: Chapman and Hall/CRC; 2016. p. 681–690.
- Krsek P, Maton B, Korman B, Pacheco-Jacome E, Jayakar P, Dunoyer C, et al. Different features of histopathological subtypes of pediatric focal cortical dysplasia. *Ann Neurol* 2008; 63: 758–69.
- Landrieu P, Husson B, Pariente D, Lacroix C. MRI-neuropathological correlations in type 1 lissencephaly. *Neuroradiology* 1998; 40: 173–6.
- Leventer RJ, Jansen A, Pilz DT, Stoodley N, Marini C, Dubeau F, et al. Clinical and imaging heterogeneity of polymicrogyria: a study of 328 patients. *Brain* 2010; 133: 1415–27.
- Li S, Jin Z, Koirala S, Bu L, Xu L, Hynes RO, et al. GPR56 regulates pial basement membrane integrity and cortical lamination. *J Neurosci* 2008; 28: 5817–26.
- Lian G, Sheen VL. Cytoskeletal proteins in cortical development and disease: actin associated proteins in periventricular heterotopia. *Front Cell Neurosci* 2015; 9: 99.
- Lu DS, Karas PJ, Krueger DA, Weiner HL. Central nervous system manifestations of tuberous sclerosis complex. *Am J Med Genet C* 2018; 178: 291–8.
- Lui JH, Hansen DV, Kriegstein AR. Development and evolution of the human neocortex. *Cell* 2011; 146: 18–36.
- Mancini G. Neuro-MIG: a European network on brain malformation. *Eur J Med Genet* 2018; 61: 41–743.
- Manikkam SA, Chetcuti K, Howell KB, Savarirayan R, Fink AM, Mandelstam SA. Temporal lobe malformations in achondroplasia: expanding the brain imaging phenotype associated with FGFR3-related skeletal dysplasias. *AJNR Am J Neuroradiol* 2018; 39: 380–4.
- Mansour S, Swinkels M, Terhal PA, Wilson LC, Rich P, Van Maldergem L, et al. Van Maldergem syndrome: further characterisation and evidence for neuronal migration abnormalities and autosomal recessive inheritance. *Eur J Hum Genet* 2012; 20: 1024–31.
- Manzini MC, Walsh CA. What disorders of cortical development tell us about the cortex: one plus one does not always make two. *Curr Opin Genet Dev* 2011; 21: 333–9.
- Martinez-Rios C, McAndrews MP, Logan W, Krings T, Lee D, Widjaja E. MRI in the evaluation of localization-related epilepsy. *J Magn Reson Imaging* 2016; 44: 12–22.
- Mata-Mbemba D, Iimura Y, Hazrati LN, Ochi A, Otsubo H, Snead OC 3rd, et al. MRI, magnetoencephalography, and surgical outcome of oligodendrocytosis versus focal cortical dysplasia type I. *AJNR Am J Neuroradiol* 2018; 39: 2371–7.
- Mellerio C, Labeyrie MA, Chassoux F, Dumas-Duport C, Landre E, Turak B, et al. Optimizing MR imaging detection of type 2 focal cortical dysplasia: best criteria for clinical practice. *AJNR Am J Neuroradiol* 2012; 33: 1932–8.

- Métin C, Alvarez C, Moudoux D, Vitalis T, Pieau C, Molnár Z. Conserved pattern of tangential neuronal migration during forebrain development. *Development* 2007; 134: 2815–27.
- Miller E, Widjaja E, Blaser S, Dennis M, Raybaud C. The old and the new: supratentorial MR findings in Chiari II malformation. *Childs Nerv Syst* 2008; 24: 563–75.
- Mirzaa G, Roy A, Dobyns WB, Millen K, Hevner RF, Hemimegalencephaly and dysplastic megalencephaly. In: H Adle-Biassette, BN Harding, JA Golden, F Gray, K Keohane, editors. *Developmental neuropathology (international society of neuropathology series)*. Hoboken, NJ: John Wiley & Sons, Ltd; 2018. p.55–61.
- Mirzaa GM, Conway RL, Gripp KW, Lerman-Sagie T, Siegel DH, DeVries LS, et al. Megalencephaly-capillary malformation (MCAP) and (MPPH) syndromes: two closely related disorders of brain overgrowth and abnormal brain and body morphogenesis. *Am J Med Genet A* 2012; 158A: 269–91.
- Mirzaa GM, Poduri A. Megalencephaly and hemimegalencephaly: breakthroughs in molecular etiology. *Am J Med Genet C Semin Med Genet* 2014; 166C: 156–72.
- Murakami JW, Weinberger E, Shaw DW. Normal myelination of the pediatric brain imaged with fluid-attenuated inversion-recovery (FLAIR) MR imaging. *AJNR Am J Neuroradiol* 1999; 20: 1406–11.
- Mutch CA, Poduri A, Sahin M, Barry B, Walsh CA, Barkovich AJ. Disorders of microtubule function in neurons: imaging correlates. *AJNR Am J Neuroradiol* 2016; 37: 528–35.
- Najm I, Sarnat HB, Blümck I. Review: the international consensus classification of Focal Cortical Dysplasia – a critical update 2018. *Neuropathol Appl Neurobiol* 2018; 44: 18–31.
- Nakano I, Funahashi M, Takada K, Toda T. Are breaches in the glia limitans the primary cause of the micropolygyria in Fukuyama-type congenital muscular dystrophy (FCMD)? Pathological study of the cerebral cortex of an FCDM fetus. *Acta Neuropathol* 1996; 91: 313–21.
- Naveed M, Kazmi SK, Amin M, Asif Z, Islam U, Shahid K, et al. Comprehensive review on the molecular genetics of autosomal recessive primary microcephaly (MCPH). *Genet Res (Camb)* 2018; 100: e7.
- Northrup H, Krueger DA, on behalf of the International Tuberous Sclerosis Complex Consensus Group. Tuberous sclerosis complex diagnostic criteria update: recommendations of the 2012 international Tuberous Sclerosis Complex Consensus Conference. *Ped Neurol* 2013; 49: 243–54.
- Oegema R, Barkovich AJ, Mancini GMS, Guerrini R, Dobyns WB. Subcortical heterotopic gray matter brain malformations: classification study of 107 individuals. *Neurology* 2019; 93: e1360–e1373.
- Oegema R, Cushion TD, Phelps IG, Chung SK, Dempsey JC, Collins S, et al. Recognizable cerebellar dysplasia associated with mutations in multiple tubulin genes. *Hum Mol Genet* 2015; 24: 5313–25.
- Pasquier B, Pécot H M, Fabre-Bocquentin B, Bensaadi L, Pasquier D, Hoffmann D, et al. Surgical pathology of drug-resistant partial epilepsy. A 10-year-experience with a series of 327 consecutive resections. *Epileptic Disord* 2002; 4: 99–119.
- Paus T, Collins DL, Evans AC, Leonard G, Pike B, Zijdenbos A. Maturation of white matter in the human brain: a review of magnetic resonance studies. *Brain Res Bull* 2001; 54: 255–66.
- Pestana Knight EM, Gonzalez-Martinez J, Gupta A. Pre-operative evaluation in pediatric patients with cortical dysplasia. *Childs Nerv Syst* 2015; 31: 2225–33.
- Pollen AA, Nowakowski TJ, Chen J, Retallack H, Sandoval-Espinosa C, Nicholas CR, et al. Molecular identity of human outer radial glia during cortical development. *Cell* 2015; 163: 55–67.
- Radner S, Banos C, Bachay G, Li YN, Hunter DD, Brunken WJ, et al. $\beta 2$ and $\gamma 3$ laminins are critical cortical basement membrane components: ablation of Lamb2 and Lamc3 genes disrupts cortical lamination and produces dysplasia. *Dev Neurobiol* 2013; 73: 209–29.
- Raybaud C, Widjaja E. Development and dysgenesis of the cerebral cortex: malformations of cortical development. *Neuroimaging Clin N Am* 2011; 21: 483–543.
- Raznahan A, Greenstein D, Lee NR, Clasen L, Giedd JN. Prenatal growth in humans and postnatal brain maturation into late adolescence. *Proc Natl Acad Sci USA* 2012; 109: 11366–71.
- Reillo I, de Juan Romero C, García-Cabezas MÁ, Borrel V. A role for intermediate radial glia in the tangential expansion of the mammalian cerebral cortex. *Cereb Cortex* 2011; 21: 1674–94.
- Ribierre T, Deleuze C, Bacq A, Baldassari S, Marsan E, Chipaux M, et al. Second-hit mosaic mutation in mTORC1 repressor DEPDC5 causes focal cortical dysplasia-associated epilepsy. *J Clin Invest* 2018; 128: 2452–8.
- Romaniello R, Arrigoni F, Fry AE, Bassi MT, Rees MI, Borgatti R, et al. Tubulin genes and malformations of cortical development. *Eur J Med Genet* 2018; 61: 744–54.
- Saito Y, Murayama S, Kawai M, Nakano I. Breached cerebral glia limitans-basal lamina complex in Fukuyama-type congenital muscular dystrophy. *Acta Neuropathol* 1999; 98: 330–6.
- Sato N, Ota M, Yagishita A, Miki Y, Takahashi T, Adachi Y, et al. Aberrant midsagittal fiber tracts in patients with hemimegalencephaly. *AJNR Am J Neuroradiol* 2008; 29: 823–7.
- Schneider JF, Vergesslich K. Maturation of the limbic system revealed by MR FLAIR imaging. *Pediatr Radiol* 2007; 37: 351–5.
- Schurr J, Coras R, Rössler K, Pieper T, Kudernatsch M, Holthausen H, et al. Mild malformation of cortical development with oligodendroglial hyperplasia in frontal lobe epilepsy: a new clinico-pathological entity. *Brain Pathol* 2017; 27: 26–35.
- Seltzer LE, Paciorkowski AR. Genetic disorders associated with postnatal microcephaly. *Am J Med Genet C Semin Med Genet* 2014; 166C: 140–55.
- Sener RN. MR demonstration of cerebral hemimegalencephaly associated with cerebellar involvement (total hemimegalencephaly). *Comput Med Imaging Graph* 1997; 21: 201–4.
- Shaheen R, Sebai MA, Patel N, Ewida N, Kurdi W, Altweijri I, et al. The genetic landscape of familial congenital hydrocephalus. *Ann Neurol* 2017; 81: 890–7.
- Silva CG, Peyre E, Nguyen L. Cell migration promotes dynamic cellular interactions to control cerebral cortex morphogenesis. *Nat Rev Neurosci* 2019; 20: 318–29.
- Smart IH. Proliferative characteristics of the ependymal layer during the early development of the mouse neocortex: a pilot study based on recording the number, location and plane of cleavage of mitotic figures. *J Anat* 1973; 116: 67–91.
- Squier W, Jansen A. Polymicrogyria: pathology, fetal origins and mechanisms. *Acta Neuropathol Commun* 2014; 2: 80.
- Stark Z, McGillivray G, Sampson A, Palma-Dias R, Edwards A, Said JM, et al. Apert syndrome: temporal lobe abnormalities on fetal brain imaging. *Prenat Diagn* 2015; 35: 179–82.
- Stutterd CA, Leventer RJ. Polymicrogyria: a common and heterogeneous malformation of cortical development. *Am J Med Genet C Semin Genet* 2014; 166C: 227–39.
- Takahara K, Morioka T, Shimogawa T, Haga S, Kameda K, Arihiro S, et al. Hemodynamic state of periictal hyperperfusion revealed by arterial spin-labeling perfusion MR images with dual postlabeling delay. *eNeurologicalSci* 2018; 12: 5–18.
- Takanashi J, Barkovich AJ. The changing MR imaging appearance of polymicrogyria: a consequence of myelination. *AJNR Am J Neuroradiol* 2003; 24: 788–93.
- Tanaka DH, Nakajima K. Migratory pathways of GABAergic interneurons when they enter the neocortex. *Eur J Neurosci* 2012; 35: 1655–60.
- Tang Y, An D, Xiao Y, Niu R, Tong X, Liu W, et al. Cortical thinning in epilepsy patients with postictal generalized electroencephalography suppression. *Eur J Neurol* 2019; 26: 191–7.

- Uccella S, Accogli A, Tortora D, Mancardi MM, Nobili L, Berloco B, et al. Dissecting the neurological phenotype in children with callosal agenesis, interhemispheric cysts and malformations of cortical development. *J Neurol* 2019; 266: 1167–81.
- Valence S, Garel C, Barth M, Toutain A, Paris C, Amsellem D, et al. RELN and VLDLR mutations underlie two distinguishable clinico-radiological phenotypes. *Clin Genet* 2016; 90: 545–9.
- Vandervore L, Stouffs K, Tanyalçin I, Vanderhasselt T, Roelens F, Holder-Espinasse M, et al. Bi-allelic variants in COL3A1 encoding the ligand to GPR56 are associated with cobblestone-like cortical malformation, white matter changes and cerebellar cysts. *J Med Genet* 2017; 54: 432–40.
- Vermeulen RJ, Wilke M, Horber V, Krägeloh-Mann I. Microcephaly with simplified gyral pattern: MRI classification. *Neurology* 2010; 74: 386–91.
- Vigliano P, Dassi P, Di Blasi C, Mora M, Jarre L. LAMA2 stop-codon mutation: merosin-deficient congenital muscular dystrophy with occipital polymicrogyria, epilepsy and psychomotor regression. *Eur J Pediatr Neurol* 2009; 13: 72–6.
- Widjaja E, Massimi L, Blaser S, Di Rocco C, Raybaud C. Midline “brain in brain”: an unusual variant of holoprosencephaly with anterior prosomeric cortical dysplasia. *Childs Nerv Syst* 2007; 23: 437–42.
- Winden KD, Yuskaitis CJ, Poduri A. Megalencephaly and macrocephaly. *Semin Neurol* 2015; 35: 277–87.
- Woods CG, Parker A. Investigating microcephaly. *Arch Dis Child* 2013; 98: 707–13.
- Yakovlev P, Wadsworth RC. Schizencephalies: a study of the congenital clefts in the cerebral mantle, I: clefts with fused lips. *J Neuropathol Exp Neurol* 1946a; 5: 116–30.
- Yakovlev P, Wadsworth RC. Schizencephalies: a study of the congenital clefts in the cerebral mantle, II: clefts with hydrocephalus and lips separated. *J Neuropathol Exp Neurol* 1946b; 5: 169–206.
- Yeung TW, Lau HY, Wong YC. Regional variation within the cerebral cortex evaluated by diffusion-weighted imaging and apparent diffusion coefficients on 1.5T and 3T magnetic resonance images. *Hong Kong J Radiol* 2013; 16: 100–9.